



# Real-time dynamic predictive cruise control for enhancing eco-driving of electric vehicles, considering traffic constraints and signal phase and timing (SPaT) information, using artificial-neural-network-based energy consumption model

Zifei Nie, Hooman Farzaneh\*

*Interdisciplinary Graduate School of Engineering Sciences, Kyushu University, Fukuoka, Japan*

## ARTICLE INFO

*Article history:*

Received 22 April 2021

Received in revised form

17 October 2021

Accepted 10 December 2021

Available online 11 December 2021

*Keywords:*

Energy efficiency

Eco-driving

Predictive cruise control

Electric vehicle

Model predictive control

Neural network model

## ABSTRACT

This paper proposes a real-time dynamic predictive cruise control (PCC) system to minimize the energy consumption for electric vehicles (EVs) under integrated traffic situations with synthetic driving scenarios, considering both constraints from the preceding vehicle and the influence of traffic signal lights. The proposed PCC system is working based on the *bi-level* model predictive control (MPC) algorithm. The Signal Phase and Timing (SPaT)-oriented MPC calculates a desired acceleration command as the optimal control signal at each sampling step based on the forthcoming SPaT information with the purpose of passing the nearest signalized intersection during the green light interval without stop. The car-following-oriented MPC executes preceding vehicle tracking task through maintaining a safe inter-distance using a customized variable time headway (VTH) strategy. The instantaneous energy consumption for EV in different traffic scenarios was quantified by a data-driven model. The developed system was validated through comparison with IDM and human driver's maneuver in both suburban and urban areas road in the city of Fukuoka, Japan, during off-peak and peak hours, using the real traffic system and SPaT data. To further evaluate the performance of the proposed PCC system in high speed driving situation, another case study with transitions from highway to urban road was conducted. The simulative results showed that the proposed PCC system can realize the energy-saving rates by 8.5%–15.6%. And it was working well and robustly under high speed driving situation.

© 2021 Elsevier Ltd. All rights reserved.

## 1. Introduction

### 1.1. Background

Transportation sector accounts for approximately 24% of global CO<sub>2</sub> emissions in 2020, and road vehicles are responsible for nearly three-quarters of transport CO<sub>2</sub> emissions [1]. Accordingly, the related international policies and low emission strategies are imperatively needed to moderate the energy and environmental burden in the transport sector. Electric vehicles (EVs) are ineluctably being adopted as a countermeasure for reducing the reliance on fossil fuels, mitigating CO<sub>2</sub> emissions and other air pollutants as well as achieving the UN's Sustainable Development Goals (SDGs)

in the transport sector [2]. According to IEA, mass popularization of electric vehicles in the road transport sector brought about 220 million barrels of oil consumption reduction in 2019, globally [3]. Although EV is one of the most promising technologies that can tackle the energy-related climate change issues, the boom in EVs will throw out radically new challenges in terms of extra energy demand in the future. The potential of renewable energy sources to power EVs can be considered as one of the key solutions. However, the biggest problem with utilizing renewable energies still remains with their intermittency and high costs. As one of the existing advanced control techniques, eco-driving proves to be a contributing strategy that can minimize energy consumption from the vehicle's driving perspective rather than enhancing the technology of the vehicle itself. The classical concept of eco-driving is based on providing the driver with optimal driving strategies, such as optimal controlling of the vehicle's speed and appropriate gear shifting decisions, to improve the fuel economy. More recently,

\* Corresponding author.

E-mail address: [farzaneh.hooman.961@m.kyushu-u.ac.jp](mailto:farzaneh.hooman.961@m.kyushu-u.ac.jp) (H. Farzaneh).

considering the influence of surrounding traffic flow and road terrain, the extension of the eco-driving concept enables road vehicles to realize better energy improvement potential.

## 1.2. Literature review

Generally, eco-driving-related research can be classified into highway-based and urban roadway-based strategies. A feedback algorithm considering powertrain and route characteristics was proposed in Ref. [4] to minimize fuel consumption in highway driving cycles. Hellström et al. used information of road terrain ahead to optimize the speed trajectory with the help of an onboard road slope database which can reduce about 3.5% fuel consumption on the 120 km route [5]. A nonlinear optimal control problem was presented by Ref. [6] to minimize fuel consumption under varying road grade profiles, indicating around 8–10% energy efficiency can be accomplished using the designed optimal velocity curve. An optimal speed profile considering the horizontal curvature for eco-driving on the curved roads was carried out, using dynamic programming (DP) algorithm in Ref. [7], indicating the proposed DP algorithm can achieve about 17.64% fuel savings compared with typical acceleration and deceleration strategy managed by other controllers. Shen et al. developed a computationally efficient algorithm based on Pontryagin's minimum principle (PMP) for EV ecological highway cruising, indicating up to 4.4% energy savings can be harvested in the uncongested real-world highway scenario [8].

Considering the impact of traffic density, urban roadway-based research can be further classified into three categories. The first one is to take into account macroscopic traffic flow, speed limitations, and road conditions. An eco-driving model based on optimal control theory was proposed by Saboohi and Farzaneh, which coordinates vehicle speed and gear ratio by aligning engine loading to diminish the fuel consumption for an intensive and unimpeded traffic flow [9]. Compared with the commonly used controllers, the model predictive control (MPC) algorithm is ingeniously used to develop more sophisticated eco-driving systems due to the superiority of handling the various traffic-imposed constraints. An energy-optimal adaptive cruise control (ACC) based on MPC and dynamic programming (DP) developed by Ref. [10] entailed a remarkable energy consumption reduction compared with the preceding vehicle on the same route, considering the speed limits, road slope, and travel time constraints. Another representative work contributed by Ref. [11] proposed a two-stage hierarchical framework for minimizing fuel consumption under the connected and automated vehicles (CAVs) environment, considering both the global traffic state variation and local driving conditions.

The second research field of eco-driving under urban transport system focuses on vehicle speed optimization using the upcoming traffic signal lights information with the advancement of Vehicle-to-Vehicle (V2V) and Vehicle-to-Infrastructure (V2I) technology. The intelligent transport system (ITS) makes it possible to engage higher levels of real-time dynamic monitoring of the vehicle performance, enabling the eco-driving system to perform better. The methodology proposed in Ref. [12] introduced a vehicle-centered predictive cruise control system that controls the vehicle based on traffic signal lights information through the ITS to reduce waiting time at the red interval of traffic signal lights and avoid unnecessarily frequent acceleration or deceleration. Their results showed that the proposed system could achieve about 41.8% of fuel economy improvement. Kamal et al. developed a comprehensive and innovative eco-driving model, using MPC, predicting the preceding vehicle speed, taking into account the changing traffic signals at intersections to improve fuel economy. Their results

revealed a significant improvement in cumulative fuel consumption compared with the conventional driving styles [13]. Minimizing idling time by implementing a velocity-planning algorithm based on probabilistic traffic signal timing models was investigated by Ref. [14], considering future knowledge of traffic signal information. Comparatively, a preliminary velocity pruning algorithm was proposed by Ref. [15], which identifies the feasible "green window" a velocity may travel along in compliance with certain road speed limits. Meng and Cassandras developed an analytical model based on the combination of parametric optimization with real-time V2I communication, in order to estimate the optimal acceleration profile for a self-driving car crossing signalized intersections [16]. An ecological ACC (Eco-ACC) architecture was presented by Ref. [17] for a plug-in hybrid electric vehicle using historical and real-time traffic signal information, which can avoid collisions from the front vehicle and compute a reference velocity that minimizes energy consumption. A recent study conducted by Ref. [18] developed an eco-driving algorithm for multiple signalized intersections, considering vehicle queues (Eco-MS-Q) algorithm to improve the fuel economy in urban areas.

The third research field focuses on eco-driving during car-following process in urban roadway, which mainly considers the constraints of the preceding vehicle. A real-time eco-driving predictive cruise control system was proposed by Ref. [19], utilizing both the information of upcoming traffic limits and the constraints from the preceding vehicle, through solving a nonlinear mixed-integer problem using Pontryagin's minimum principle and bisection method. Nie and Farzaneh proposed an advanced ACC system for eco-driving, which dynamically computes an optimal acceleration command as an input to the host vehicle to realize the eco-driving strategy while tracking the preceding vehicle, as well as obtaining the objectives of driving safety and comfortability [20]. Zhou et al. developed a reinforcement-learning-based car-following model for CAVs, in order to improve the fuel economy at the signalized intersection [21]. However, the circumstance for a mixed traffic flow with CAVs and manually driven vehicles (MVs) was not considered in their study. A quantitative servo-loop Pulse-and-Gliding (PnG) strategy was implemented in an ACC system based on V2V technology by Ref. [22] to realize the minimization of fuel consumption of the host vehicle by 20%, while maintaining a more accurate inter-distance to the preceding vehicle. An Eco-ACC controller designed in Ref. [23] based on the nonlinear model predictive control on a Plug-in hybrid electric vehicle (PHEVs) showed about 19% energy saving, through optimally adjusting the vehicle speed and the behavior of the preceding vehicle. Ojeda et al. developed a real-time eco-driving strategy based on optimal control problem (OCP) for automated EV, which can guarantee 11.83% of energy savings, considering the risk of accident with the preceding vehicle [24].

As the premise to evaluate the performance of the eco-driving system, it is important to develop an energy consumption estimation model with high accuracy. Current existing research about vehicle energy consumption estimation mainly focused on conventional internal combustion engine vehicles (ICEVs). From the perspective of the model inputs, Huanyu Yue categorized the fuel consumption model into micro-, meso-, and macroscopic models according to the scale of input [25]. Mesoscopic models consider the influence on fuel consumption from different driving modes. The fuel consumption estimated by the macroscopic models is based on traveling time, distance and averaged driving velocity, which leads to the limited estimation accuracy. The microscopic fuel consumption models are obtained using engine power or engine torque, which can guarantee the estimation accuracy only under the steady driving state. To make up for the shortcomings,

Zhou and Jin [26] proposed the scheme of “steady-state estimation + transient correction” to estimate the instantaneous energy consumption more accurately.

Currently, research work about applying the data-driven model to estimate the energy consumption for electric vehicles is limited, which handicaps the development of energy-efficient driving strategies for EVs. A neural network was trained [27] in order to estimate the energy consumption of electric vehicles considering the driving behavior. The chosen input features to the neural network model are velocity, acceleration and jerk. The output of the proposed estimation model is the remaining battery charge. However, the main input features are selected to represent the driving behavior. Therefore, the vehicle dynamics characteristics are not considered for the energy consumption estimation. A deep convolutional neural network-based solution was developed [28] for the estimation of energy consumption of EVs, considering three external parameters, including road elevation, tractive effort, and driving velocity. Through multiple tests and exploration, a CNN model with seven layers was performed well using the image converted from time-series data. Although, this model features high estimation accuracy, real-time acquisition of the road elevation data is problematic for the model application in eco-driving system development. It is relatively easier to acquire the motor torque and motor speed data in real-time, which feedback the influence from road gradient to the vehicle dynamics characteristic indirectly. In this research, it is assumed that the EVs share the same vehicle longitudinal dynamics with the ICEVs, and the energy conversion of EVs is much higher and more direct. Therefore, guided by the modeling scheme of fuel consumption estimation of ICEVs, this research applies machine learning to develop a new instantaneous energy consumption estimation model based on the strong mapping relationship between energy consumption and EV's state variables and dynamic characteristics, laying the foundation for developing the predictive cruise control system for Enhancing Eco-driving of Electric Vehicles. The recent representative research works are listed in Table 1.

### 1.3. Research gap and originality highlights

Based on the above review, most of the previous research works focused on a specific single driving scenario to improve the fuel/energy economy, namely, considering the influence of either (1) only car-following behavior, or (2) only upcoming traffic signal lights without interaction from surrounding vehicles. Yet, the actual daily urban traffic situation covers both car-following and interaction with traffic signal lights. For example, a vehicle starts and quickly accelerates to the allowable speed limit of the road section. However, due to the increase of traffic flow, it has to follow the preceding vehicle. With the decrease of traffic flow, the preceding vehicle may change lanes, making the host vehicle consider the traffic signal lights at the intersection ahead and ready to stop at the red light interval. Therefore, to enhance energy efficiency for the overall driving task, it is necessary to automatically and smoothly deal with various driving scenarios.

To fill the existing gap in previous studies, a predictive cruise control system in this research is developed to handle the integrated multiple driving scenarios with combined constraints of both car-following situations and traffic signal lights timing and phase through: (1) energy-efficient deceleration when there is an inevitable stop in front of the red intervals of the traffic lights; (2) car-following situation when a preceding vehicle is driving within the range of the onboard sensors; (3) optimal vehicle velocity dynamic control using the upcoming traffic signal lights information as long as without any preceding vehicles in the detection range of onboard sensors.

In this study, a *bi-MPC* architecture (a Car-following-oriented MPC and a SpaT-oriented MPC) is designed to realize the proposed predictive cruise control system. The objective function of the MPCs is minimization of the energy consumption of the EV in a given traffic condition. An Artificial Neural Network (ANN)-based energy consumption model combined with the vehicle dynamics model is developed to predict the instantaneous energy consumption of the EV, taking into account the technical

**Table 1**  
A review of recent studies on eco-driving.

Research purpose	Modeling approach	Achievements	Ref.
To improve fuel economy while maintaining a safe following distance	Car-following-oriented MPC	Maintaining a safe distance between leading vehicle while obtaining fuel economy	[29]
To reduce fuel consumption and emissions, considering the car-following scenario	Model predictive multi-objective control framework	Fuel consumption can be reduced by 10.49% with the proposed controller compared with conventional controllers in Advanced Vehicle Simulator (ADVISOR)	[30]
To improve fuel economy under the vehicle-to-vehicle communication structure	Ecological cooperative adaptive cruise control (eCACC) strategy	Better car-following performance results in significant energy savings in different driving cycles	[31]
To improve fuel economy of the vehicle driving by incorporating traffic information into the energy management strategies	Deep deterministic policy gradients approach	Fuel economy improvement, by taking traffic information into account	[32]
To realize better power allocation of hybrid EV and optimize the fuel economy	Fuzzy adaptive PMP optimization	Fuel economy improvement and maintaining the state of charge of battery	[33]
To enhance eco-driving in the urban traffic system, considering multiple signalized intersections	Open-loop optimal control problem (OCP) combined with three-stage operation rules and Dijkstra algorithm	About 10.14% and 5.04% fuel consumption reduction can be achieved for the urban and suburban area, respectively	[34]
Eco-speed trajectory planning in real-time considering upcoming traffic and road constraints	Energy Adaptive Cruise Control (EACC) based on MPC in the space domain	The proposed MPC achieves 2.5% more energy savings than linear MPC in the time domain	[35]
To improve fuel economy and air quality in a traffic system with signalized intersections in the city of Riverside, CA, USA	Cooperative eco-driving (CED) system with a role transition protocol	About 7% reduction in energy consumption and 59% reduction in pollution emission can be achieved, using full utilization of the connected and autonomous vehicles (CAVs)	[36]
To improve fuel economy for CAV platoon driving through successive signalized intersections	Ecological cooperative adaptive cruise control (Eco-ACC) based on the combination of DP and OCP approaches	About 8.02% improvement in fuel economy and 2.92% reduction in trip time can be achieved	[37]
To enhance CAVs eco-driving control on signalized roadways	MPC algorithm with traffic management strategies and road geometry constraints, using Distributionally Robust Chance Constraint (DRCC)	About 23.6% energy savings through Smooth trajectories generation with shorter idling time at the intersection	[38]

characteristics of the given driving cycle and powertrain. A real-time dynamic switch logic is precisely designed to execute the selection between two MPCs so that the vehicle can operate in an energy-efficient manner at every time step, i.e., realize the motion tracking of the preceding vehicle while under the influence of upcoming traffic signal lights information. The SPaT-oriented MPC computes an optimal control sequence at each time step based on the forthcoming signal phase and timing information to pass the nearest signalized intersection during the green interval. It is assumed that the SPaT information provided by the ITS can be perceived in real-time by the host vehicle. A trigonometric speed profile is applied when a stop at a red light is unavoidable. The car-following-oriented MPC carries out preceding vehicle tracking task, by maintaining a safe inter-distance using a novel variable time headway (VTH), considering the relative velocity between the host and preceding vehicles. The performance of the proposed real-time dynamic PCC system is amply analyzed through three typical real case studies in Fukuoka, Japan. Finally, the potential of energy savings and emissions reduction from the proposed PCC system is evaluated.

The following main contributions can be highlighted:

- 1) A real-time dynamic PCC system with bi-level MPC framework is developed to minimize energy consumption and driving safety of the EV. To the best of our knowledge, this was the first study in which a neural network model, instead of an explicit model, was combined with the MPC algorithm applying to the eco-driving control problem.
- 2) A real-time updated switch logic is proposed to automatically differentiate driving scenarios so that either the car-following-oriented or SPaT-oriented MPC can be selected for every time step.
- 3) A customized VTH strategy considering the relative velocity between host and preceding vehicle is designed within the car-following model predictive controller to guarantee driving safety and traffic flow stability.
- 4) Instead of using the traditional knowledge-based energy consumption estimation model, a new artificial-neural-network-based instantaneous energy consumption model (ANN-IECM), based on the strong mapping relationship between energy consumption and EV's state variables, was developed and used

to predict the energy economy performance of the EV with proposed PCC system.

- 5) The superiority of the proposed PCC was evaluated compared with both human driver and intelligent driver models.
- 6) The simulation case studies are conducted with access to real traffic signal phasing and timing data in suburban and urban areas in Fukuoka, Japan, under the different traffic systems.

The remaining of this paper is organized as follows: The problem formulation and system modeling are presented in Section 2, including SPaT-Oriented MPC algorithm, Car-following-Oriented MPC algorithm, the switch logic algorithm, a novel VTH strategy, the vehicle longitudinal dynamic model, and the original ANN-based instantaneous energy consumption estimation model. Section 3 shows the overall results and discussion. Conclusions and the future prospect are included in Section 4.

## 2. Problem formulation and system modeling

### 2.1. Predictive cruise control system formulation based on MPC algorithm

This research aims to develop a real-time dynamic predictive cruise control (PCC) system to minimize the energy consumption for EVs in the typical urban traffic system, considering both constraints from the preceding vehicle and the influence of traffic signal lights. The proposed method is illustrated in Fig. 1.

$d_{rel}$  denotes the inter-distance between host and preceding vehicles;  $d_{TL}$  denotes the relative distance to the upcoming signalized intersection.

**SPaT-Oriented MPC:** Assume the host vehicle is equipped with onboard sensors and performs real-time bi-directional wireless communication with infrastructure components, such as traffic signal lights. If onboard sensors of the host vehicle couldn't detect the preceding vehicle, the host vehicle, at this instant, is supposed to be driven by an eco-speed that is optimized through real-time traffic SPaT information to cross the upcoming signalized intersection during its green interval. However, consider a stop in front of a red interval is inevitable; then, the host vehicle is expected to follow a smooth speed trajectory planned by trigonometric speed profiles to slow down the vehicle to the stop in an energy-efficient way.

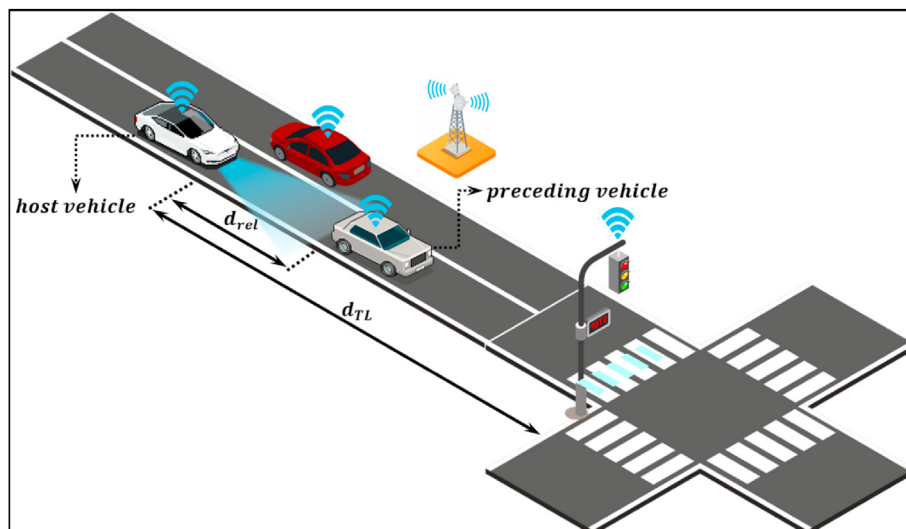


**Fig. 1.** Illustration of the proposed predictive cruise control system.

**Car-following-Oriented MPC:** If the preceding vehicle is within the detection range of onboard sensors, the host vehicle is supposed to track the preceding vehicle, while maintaining a safe and high-road-resource-utilization rate inter-distance ( $d_{rel}$ ) to the preceding vehicle.

The detailed modeling approach used in both MPCs is explained as follows:

### 2.1.1. SPA-T-oriented model predictive control algorithm

The SPA-T-Oriented MPC is designed to handle the traffic scenario with no preceding vehicle in the range of onboard sensors, computing an optimal control command for the host vehicle to cross the upcoming signalized intersection without any stop, by accessing real-time traffic SPA-T information. The objective function for this SPA-T-Oriented MPC controller is expressed as follow:

$$\mathcal{J}_{\text{SPA-T-Oriented MPC}} = \sum_{i=k}^{k+N_e-1} \left( E(v_{host,i}, a_{host,i}, T_{m,i}, \omega_{m,i}) + \varphi_1 (v_{host,i} - v_{target})^2 + \varphi_2 \varepsilon_{1,i}^2 + \varphi_3 \varepsilon_{2,i}^2 \right) \quad (1)$$

where,  $E$  refers to the instantaneous energy consumption of the host vehicle, which is a function mapping of host vehicle velocity ( $v_{host,i}$ ), acceleration ( $a_{host,i}$ ), an its motor torque ( $T_{m,i}$ ) and speed ( $\omega_{m,i}$ ).  $v_{target}$  represents the reference target vehicle velocity optimized by SPA-T information.  $\varepsilon_{1,i}$  and  $\varepsilon_{2,i}$  are the relaxation factors.  $\varphi_1$ ,  $\varphi_2$ , and  $\varphi_3$  are weighting factors, respectively.

Considering the above objective function, the proposed MPC can be transformed into a linearly constrained quadratic programming (QP) problem, which solves the following optimization problem from the current control step  $k$  over one control horizon  $N_e$ .

$$\begin{aligned} \min & \sum_{i=k}^{k+N_e-1} \left( E(v_{host,i}, a_{host,i}, T_{m,i}, \omega_{m,i}) + \varphi_1 (v_{host,i} - v_{target})^2 \right. \\ & \left. + \varphi_2 \varepsilon_{1,i}^2 + \varphi_3 \varepsilon_{2,i}^2 \right) \end{aligned} \quad (2)$$

s.t.

$$\begin{aligned} v_{host,i+1} = & v_{host,i} + \frac{1}{m_{eq}} \left[ i_g \cdot \eta_e \cdot \frac{T_{m,i}}{r_w} - c_r \cdot m_{eq} \cdot g \cdot \cos \theta_i \right. \\ & \left. - \frac{1}{2} \cdot \rho_a \cdot A_f \cdot C_D \cdot v_{host,i}^2 - m_{eq} \cdot g \cdot \sin \theta_i \right] \end{aligned} \quad (3)$$

$$d_{TL,i+1} = d_{TL,i} - \frac{v_{host,i} + v_{host,i+1}}{2} \quad (4)$$

$$0 \leq d_{TL,i} \leq d_{TL,max} + \varepsilon_{1,i} \quad (5)$$

$$v_{min,i} \leq v_{host,i} \leq v_{max,i} \quad (6)$$

$$a_{min,i} \leq a_{host,i} \leq a_{max,i} \quad (7)$$

$$j_{min,i} - \varepsilon_{2,i} \leq a_{host,i+1} - a_{host,i} \leq j_{max,i} + \varepsilon_{2,i} \quad (8)$$

$$0 \leq T_{m,i} \leq T_{m,max} \quad (9)$$

$$0 \leq \omega_{m,i} \leq \omega_{m,max} \quad (10)$$

where  $m_{eq}$  is the equivalent total mass of the vehicle;  $i_g$  is the gear

ratio of the single transmission;  $\eta_e$  represents the total mechanical efficiency of the driveline;  $r_w$  refers to the radius of the vehicle wheel;  $c_r$  is the rolling resistance coefficient;  $g$  denotes the gravitational acceleration;  $\theta$  refers to the road gradient;  $\rho_a$  is the air density;  $A_f$  refers to the frontal area of the vehicle;  $C_D$  denotes the aerodynamic drag coefficient.

The overall control problem is established based on the vehicle longitudinal dynamic model explained in the next section. The objective function to be minimized, consists of four terms for different control objectives. The first term to be minimized is the instantaneous energy consumption ( $E$ ) of the host vehicle, during the given traffic system. If the first term is only existing, the host vehicle would have no motivation to move because the first term forces the host vehicle to consume as little energy as possible. Therefore, the second term is needed to penalize the difference between host vehicle velocity and reference target vehicle velocity, so that the host vehicle can track the reference target velocity to minimize the energy consumption further. The third term penalizes the relaxation factor  $\varepsilon_1$  enforcing the host vehicle to approach the stop bar as close as possible, while performing an evitable stop at the red interval. The fourth term is introduced with the relaxation factor  $\varepsilon_2$  to minimize the jerk,  $j$ , so that the driving comfortability can be guaranteed. The host vehicle velocity is calculated by constraint (3), and constraint (4) obtains the distance to the signalized intersection, with a soft constraint (5) to avoid the active stop far from the signalized intersection. The vehicle velocity is bounded with the road section speed limitation in constraint (6), and vehicle acceleration, jerk, motor torque, and motor speed are all limited by the technical characteristics of the vehicle itself in constraints (7) to (10), respectively. After solving the above optimization problem in each time step, a control sequence can be obtained. The first element of the control sequence is used as the actual control input command to the host vehicle. The overall process above is then repeated to achieve the real-time updated target speed tracking to minimize energy consumption.

### 2.1.2. Car-following-oriented model predictive control algorithm

The car-following-oriented MPC is developed to manage the traffic scenario with the preceding vehicle in the detection range of onboard sensors. Similarly, the MPC problem is formulated into another linearly constrained QP problem, as follow

$$\begin{aligned} \mathcal{J}_{\text{Car-following Oriented MPC}} = & \sum_{i=k}^{k+N_e-1} \left( E(v_{host,i}, a_{host,i}, T_{m,i}, \omega_{m,i}) \right. \\ & \left. + \varphi_1 \varepsilon_{1,i}^2 + \varphi_2 \varepsilon_{2,i}^2 + \varphi_3 \varepsilon_{3,i}^2 \right) \end{aligned} \quad (11)$$

$$\begin{aligned} \min & \sum_{i=k}^{k+N_e-1} \left( E(v_{host,i}, a_{host,i}, T_{m,i}, \omega_{m,i}) + \varphi_1 \varepsilon_{1,i}^2 + \varphi_2 \varepsilon_{2,i}^2 + \varphi_3 \varepsilon_{3,i}^2 \right) \end{aligned} \quad (12)$$

s.t.

$$\begin{aligned} v_{host,i+1} = & v_{host,i} + \frac{1}{m_{eq}} \left[ i_g \cdot \eta_e \cdot \frac{T_{m,i}}{r_w} - c_r \cdot m_{eq} \cdot g \cdot \cos \theta_i \right. \\ & \left. - \frac{1}{2} \cdot \rho_a \cdot A_f \cdot C_D \cdot v_{host,i}^2 - m_{eq} \cdot g \cdot \sin \theta_i \right] \end{aligned} \quad (13)$$

$$d_{TL,i+1} = d_{TL,i} - \frac{v_{host,i} + v_{host,i+1}}{2} \quad (14)$$

$$0 \leq d_{TL,i} \leq d_{TL,max} + \epsilon_{1,i} \quad (15)$$

$$v_{min,i} \leq v_{host,i} \leq v_{max,i} \quad (16)$$

$$a_{min,i} \leq a_{host,i} \leq a_{max,i} \quad (17)$$

$$j_{min,i} - \epsilon_{2,i} \leq a_{host,i+1} - a_{host,i} \leq j_{max,i} + \epsilon_{2,i} \quad (18)$$

$$0 \leq T_{m,i} \leq T_{m,max} \quad (19)$$

$$0 \leq \omega_{m,i} \leq \omega_{m,max} \quad (20)$$

$$v_{rel,i} = v_{preceding,i} - v_{host,i} \quad (21)$$

$$D_{safe,i} = \tau_1 \cdot v_{host,i} + \tau_2 \cdot v_{host,i}^2 - \tau_3 \cdot v_{rel,i} \cdot v_{host,i} + d_{min} \quad (22)$$

$$d_{rel,i+1} = d_{rel,i} + \left( \frac{v_{preceding,i} + v_{preceding,i+1}}{2} - \frac{v_{host,i} + v_{host,i+1}}{2} \right) \quad (23)$$

$$D_{safe,i} \leq d_{rel,i} \leq D_{safe,i} + \epsilon_{3,i} \quad (24)$$

where  $\epsilon_3$  represents the relaxation factor;  $v_{preceding}$  refers to the velocity of the preceding vehicle;  $D_{safe}$  refers to the dynamic, safe distance between host and preceding vehicle;  $d_{min}$  refers to the minimum inter-distance when two vehicles are motionless;  $\tau_1$ ,  $\tau_2$ , and  $\tau_3$  are constant values that are greater than zero.

The optimization problem within the car-following oriented MPC shares a similar objective with the previous one. Instead of constraining the velocity of the host vehicle approaching the reference target velocity, another relaxation factor  $\epsilon_3$  is introduced to maintain the safe inter-distance between host and preceding vehicle during the car-following process. The relative velocity between two vehicles is calculated by constraint (21), which is further applied to calculate the dynamic safe inter-distance between two vehicles by constraint (22). Real-time relative distance  $d_{rel}$  is calculated by constraint (23). The driving safety is guaranteed by constraint (24), which also includes a soft constraint motivating the host vehicle moving forward to realize the function of car-following. Once the  $d_{rel}$  is greater than  $D_{safe}$ , the relaxation factor  $\epsilon_3$  increases to motivate the host vehicle to drive faster.

Considering the driving safety, and road utilization, the safe inter-distance between the host and preceding vehicle can be calculated as follows [39]:

$$D_{safe} = CTH \cdot v_{host} + d_{min} \quad (25)$$

where  $CTH$  represents the constant time headway.

In this research, instead of adopting the constant time headway ( $CTH$ ), a customized variable time headway ( $VTH$ ) strategy is designed, taking into account not only the velocity of the host vehicle but also the relative velocity between host and preceding vehicle, which is expressed as follow:

$$VTH = \tau_1 + \tau_2 \cdot v_{host} - \tau_3 \cdot v_{rel} \quad (26)$$

$$v_{rel} = v_{preceding} - v_{host} \quad (27)$$

where  $v_{rel}$  refers to the relative velocity between host and preceding vehicle;  $\tau_1$ ,  $\tau_2$ , and  $\tau_3$  are constants greater than 0. Substituting the customized  $VTH$  for  $CTH$  in the above expression, an adaptive safe inter-distance can be obtained as follow:

$$D_{safe} = VTH \cdot v_{host} + d_{min} = \tau_1 \cdot v_{host} + \tau_2 \cdot v_{host}^2 - \tau_3 \cdot v_{rel} \cdot v_{host} + d_{min} \quad (28)$$

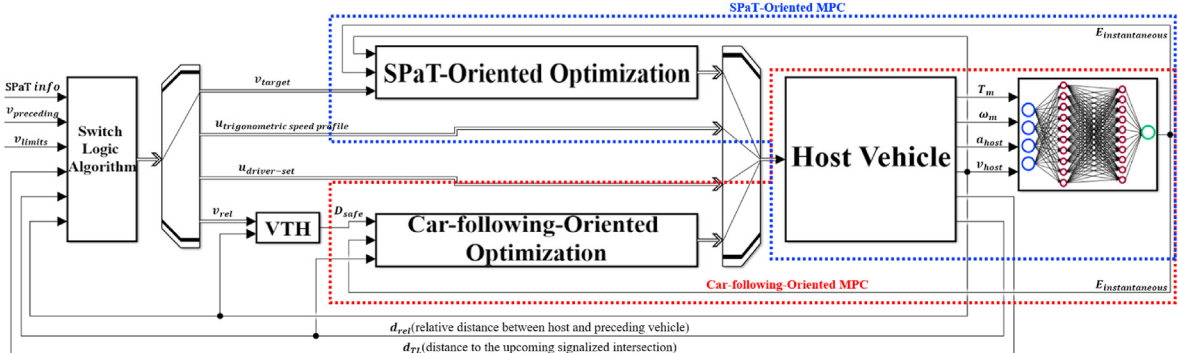
### 2.1.3. Switch logic algorithm

The schematic of the proposed predictive cruise control system simulation model, which is developed in MATLAB/Simulink, is depicted in Fig. 2.

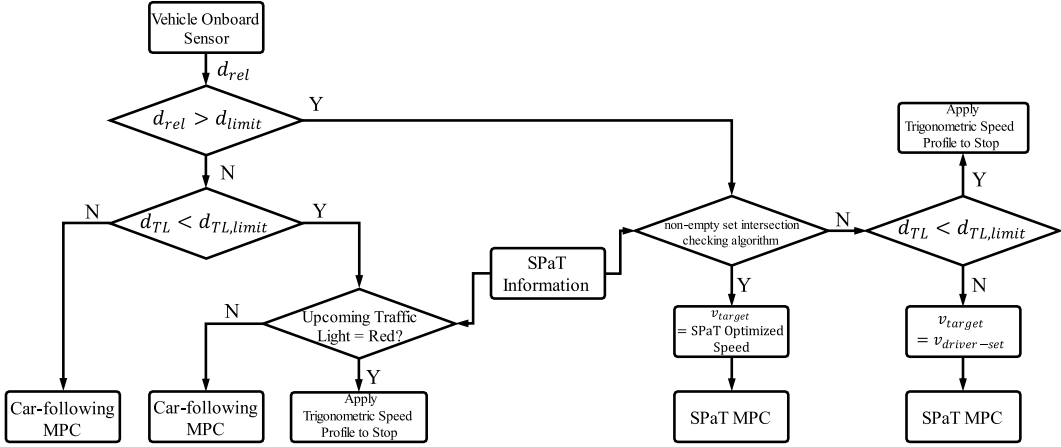
The core functional block consists of two linear model predictive controllers, the car-following-oriented MPC and the SPaT-oriented MPC. The optimized control command  $u$ , as input to the host vehicle, is calculated for each time step by either of these two controllers. The instantaneous outputs obtained from the host vehicle block, including its velocity  $v_{host}$ , inter-vehicle distance  $d_{rel}$ , and the relative distance to the nearest signalized intersection  $d_{TL}$ , together with real-time traffic signal phasing and timing information, the velocity of preceding vehicle  $v_{pre}$ , and speed limits on the certain road section  $v_{limits}$ , are used to be fed into the switch logic algorithm to select one of two MPCs properly. The detailed switch logic algorithm is further presented in Fig. 3.

For each time step, the following decision making process will be conducted by the proposed switch logic algorithm:

- Compare the detected  $d_{rel}$  with a limited value  $d_{limit}$ ;
- If  $d_{rel}$  is no greater than  $d_{limit}$ , the switch logic will further compare the current distance to the upcoming signalized intersection  $d_{TL}$  with a limited value  $d_{TL,limit}$ ;



**Fig. 2.** Schematic of data flow within the proposed predictive cruise control system.

**Fig. 3.** Flow diagram of the Switch logic algorithm.

- If  $d_{TL}$  is greater than  $d_{TL,limit}$ , the Car-following Oriented MPC will be selected to control the host vehicle to follow the preceding vehicle;
- If  $d_{TL}$  is less than  $d_{TL,limit}$ , the switch logic algorithm will further check if the upcoming traffic light is red;
- If it is not red, then Car-following Oriented MPC will be selected to control the host vehicle to follow the preceding vehicle; if it is red, then the host vehicle stops tracking the preceding vehicle and prepares using current velocity to stop in an energy-efficient manner by applying the trigonometric speed profile at the traffic light;
- If  $d_{rel}$  is greater than  $d_{limit}$ , the switch logic will apply the “non-empty set intersection checking algorithm” to find possible velocity range;
- If found, the target velocity for the host vehicle will be assigned by a SPaT optimized Speed and SPaT Oriented MPC will be selected;
- If not found, the switch logic will compare the current distance to the upcoming signalized intersection  $d_{TL}$  with a limited value  $d_{TL,limit}$ :
- If  $d_{TL}$  is greater than  $d_{TL,limit}$ , the target velocity for the host vehicle will be assigned by a driver-set velocity and SPaT Oriented MPC will be selected;
- If  $d_{TL}$  is less than  $d_{TL,limit}$ , it means that passing the upcoming signalized intersection without any stop using current velocity is impossible; then, the host vehicle will prepare to stop in an energy-efficient manner by applying the trigonometric speed profile at the traffic light.

The critical variable determining the selection between two MPCs is the real-time inter-distance between host and preceding vehicle,  $d_{rel}$ . On the one hand, if  $d_{rel}$  is no less than the onboard sensor limit detection range,  $d_{limit}$ , then a non-empty set intersection checking algorithm based on a set of logical rules is applied to find an optimal reference vehicle velocity. If a vehicle plans to cross the first green interval of the upcoming traffic signal light at the current time step, its velocity should be firstly within the range [12]:

$$\left[ \frac{d_{TL}}{r_1}, \frac{d_{TL}}{g_1} \right] \quad (29)$$

where  $r_1$  and  $g_1$  denote the start time of the first red and green interval of the nearest upcoming traffic signal light, respectively. Secondly, the feasibility of crossing the signalized intersection

depends on if the above range has the intersection with the allowable speed limits on a certain road section  $[v_{min}, v_{max}]$ . If the “set intersection is empty”, the set intersection with the following green interval will be checked until a non-empty set intersection can be found. The mathematical expression of this “non-empty set intersection checking algorithm” is represented by Ref. [12]:

$$\left[ \frac{d_{TL}}{r_i}, \frac{d_{TL}}{g_i} \right] \cap [v_{min,i}, v_{max,i}] \quad (30)$$

Then, the optimal reference vehicle velocity  $v_{target}$  at each time step can be obtained by the following equation:

$$v_{target} = \max \left\{ \left[ \frac{d_{TL}}{r_i}, \frac{d_{TL}}{g_i} \right] \cap [v_{min,i}, v_{max,i}] \right\} \quad (31)$$

Subsequently, the SPaT-Oriented MPC is selected to track the  $v_{target}$  and compute a future control sequence  $\{u^1(i), u^2(i), \dots, u^k(i)\}$  that optimizes the objective function in Eq. (1). Wherein, the first control command  $u^1(i)$  is applied as the input to the host vehicle. The relationship between the input control command  $u(i)$  and vehicle acceleration  $a(i)$  can be approximated by the first-order dynamic response:

$$\lambda \frac{da(i)}{di} + a(i) = u(i) \quad (32)$$

where  $\lambda$  represents the time lag corresponding to the finite bandwidth of the vehicle's dynamic response; adopting the difference approximation method, the above equation can be described as:

$$\lambda \frac{a(i+1) - a(i)}{T_s} + a(i) = u(i) \quad (33)$$

where  $T_s$  refers to the sampling time period.

If a non-empty set intersection is nonexistent instead, which means that a stop at the upcoming signalized intersection is inevitable, then the distance to the upcoming signalized intersection,  $d_{TL}$ , will be compared with the limit relative distance to the upcoming signalized intersection,  $d_{TL,limit}$ . If  $d_{TL}$  is greater than  $d_{TL,limit}$ , the driver set velocity will be assigned to  $v_{target}$ , until  $d_{TL}$  exceeds  $d_{TL,limit}$ . Once  $d_{TL}$  becomes smaller than  $d_{TL,limit}$ , a trigonometric speed profile is applied to obtain an energy-efficient and driving-comfort-ensured reference speed as  $v_{target}$ , by limiting the jerk at each time step [40]. Fig. 4 shows the trigonometric speed profile that decelerates to the stop.

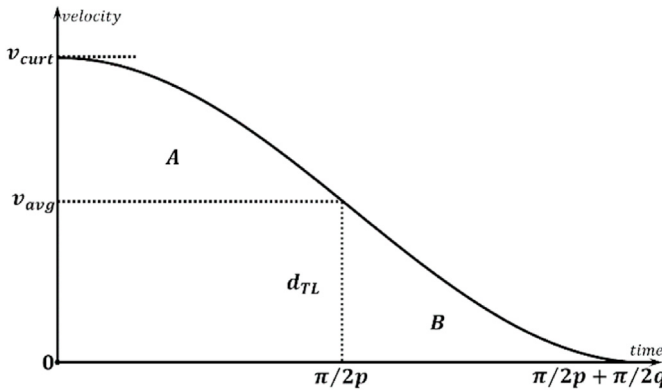


**Fig. 4.** Deceleration-to-a-stop profile of the piecewise trigonometric-linear function.

The mathematical expression is shown as below:

$$v = \begin{cases} v_{avg} + v_r \cos(pt), t \in [0, \frac{\pi}{2p}] \\ v_{avg} + v_r \cdot \frac{p}{q} \cdot \cos\left[q\left(t - \frac{\pi}{2p} + \frac{\pi}{2q}\right)\right], t \in [\frac{\pi}{2p}, \frac{\pi}{2p} + \frac{\pi}{2q}] \end{cases} \quad (34)$$

$$v_{avg} = \frac{d_{TL}}{t^{arr}} \quad (35)$$

$$v_r = v_{curt} - v_{avg} \quad (36)$$

where  $v_{avg}$  is the possible average velocity required to reach the target stop bar at a specific time instant;  $t^{arr}$  denotes the time required to reach the target stop bar;  $v_r$  represents the difference between the current velocity of the vehicle  $v_{curt}$ , and possible average velocity,  $v_{avg}$ ;  $p$  and  $q$  refer to the determinants which regulate the rate of change of deceleration, the jerk, in region A and B respectively. The value of  $q$  is decided based on the given value of  $p$ , by the following formula [40]:

$$q = \frac{1}{2} \left[ -p\left(\frac{\pi}{2} - t^{arr} \cdot p\right) + \sqrt{p^2\left(\frac{\pi}{2} - t^{arr} \cdot p\right)^2 - 4p^2\left(\frac{\pi}{2} - 1\right)} \right] \quad (37)$$

To achieve driving comfortability and minimize energy consumption,  $q$  and  $p$  are constrained as follows:

$$-2.5m/s^2 \leq q \leq 2.5m/s^2 \quad (38)$$

$$-10m/s^3 \leq v_r \cdot p \cdot q \leq 10m/s^3 \quad (39)$$

Once the  $v_{target}$  is assigned by the reference speed obtained from the above trigonometric speed profiles, the SPaT-Oriented MPC will be selected to track the desired  $v_{target}$ , until the host vehicle stops at the stop bar of the signalized intersection. On the other hand, for some specific time instant, if  $d_{rel}$  is not greater than the onboard sensor limit detection range,  $d_{limit}$ , then, the car-following-oriented MPC will be selected to maintain a safe, comfortable, and efficient road-resources-use inter-vehicle spacing based on a customized variable time headway strategy.

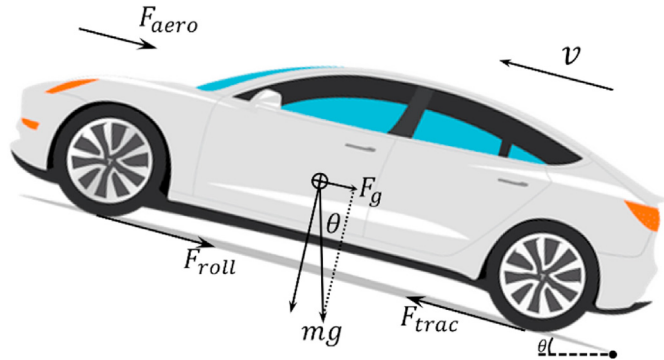


**Fig. 5.** Longitudinal forces acting on a vehicle driving on a tilted road.

## 2.2. Vehicle longitudinal dynamics model

The longitudinal vehicle dynamics are modeled based on the sum of all forces acting in the longitudinal direction illustrated in Fig. 5.

According to the Newton's second law of motion, the longitudinal acceleration of the host vehicle  $a_{host}$  is calculated as follows:

$$a_{host}(t) = \frac{dv_{host}(t)}{dt} = \frac{1}{m_{eq}} [F_{trac}(t) - \sum F_{res}(t)] \quad (40)$$

where  $F_{trac}$  represents the traction force, and  $F_{res}$  collectively refers to the resistance forces from different aspects.

The powertrain of the electric vehicle consists of the battery pack, a DC-AC converter, an electric motor, and a single ratio transmission. The electrical energy is converted to mechanical energy delivered to the wheels through a single gear ratio gearbox. Accordingly, the traction force  $F_{trac}$  can be further expressed as:

$$F_{trac}(t) = i_g \cdot \eta_e \frac{T_m(t)}{r_w} \quad (41)$$

The resistance forces  $F_{res}$  includes rolling resistance  $F_{roll}$ , aerodynamic drag force  $F_{aero}$ , and gradient resistance  $F_g$ , which can be expressed as follows:

$$\sum F_{res}(t) = F_{roll}(t) + F_{aero}(t) + F_g(t) \quad (42)$$

The rolling resistance  $F_{roll}$ , concerned with rolling resistance coefficient  $c_r$ , can be further calculated by the following equation:

$$F_{roll}(t) = c_r \cdot m_{eq} \cdot g \cdot \cos \theta(t) \quad (43)$$

The aerodynamic drag force  $F_{aero}$ , related with air density  $\rho_a$ , the frontal area of the vehicle  $A_f$ , and aerodynamic drag coefficient  $C_D$ , is the function of the longitudinal vehicle speed, which can be calculated as follows:

$$F_{aero}(t) = \frac{1}{2} \rho_a \cdot A_f \cdot C_D \cdot v_{host}^2(t) \quad (44)$$

The gradient resistance  $F_g$ , due to the gravity when driving on an uphill road, can be calculated by:

$$F_g(t) = m_{eq} \cdot g \cdot \sin \theta(t) \quad (45)$$

By integrating the equations mentioned above, the motor torque  $T_m$  and motor speed  $\omega_m$  are obtained as follows:

$$T_m(t) = \frac{(a_{host}(t) \cdot m_{eq} + \sum F_{res}(t))}{i_g \cdot \eta_e} \quad (46)$$

$$\omega_m(t) = i_g \cdot \omega_w(t) = i_g \cdot \frac{\nu_{host}(t)}{r_w} \quad (47)$$

### 2.3. Instantaneous energy consumption model based on artificial neural network

The previous studies indicate that, the motor torque and motor speed are required to reflect the impact of road slope variation on energy consumption [41,42]. Additionally, the vehicle velocity and acceleration are essential features to reflect the transient energy consumption. The EV chassis dynamometer experiments are generally needed to acquire the data, including vehicle speed, acceleration, motor torque, and motor speed. In this study, a simulated chassis dynamometer for electric vehicles is developed through co-simulation of CarSim and MATLAB/Simulink, using the hatchback electric vehicle dynamic model, shown in Fig. 6. The input data are two different standard driving cycles, the steady-state driving cycle, and the US06 driving cycle available from Ref. [43]. Corresponding output data, including longitudinal vehicle acceleration ( $m/s^2$ ), motor output torque ( $N\cdot m$ ), motor speed (rpm), and instantaneous energy consumption ( $W \cdot 0.1s$ ), are

collected by data logger with a sampling period of 0.1s.

The collected sample data, further used to train the ANN-based instantaneous energy consumption model, are merged, shuffled, normalized, and grouped into the training set, validation set, and test set. The sample data, including inputs, vehicle velocity, acceleration, motor torque, and motor speed, and output, instantaneous energy consumption, are visualized in Fig. 7.

The multilayer artificial neural networks with a highly recommended supervised algorithm – Levenberg-Marquardt back-propagation training algorithm are constructed as Fig. 8. According to Ref. [44], the universal approximation capabilities of networks with two hidden layers are substantiated. Consequently, in this paper, the network with two hidden layers is defined.

The overall training algorithm proceeds as follows: first, the training dataset is fed into the neural network allocated with different weights and biases; second, the estimation of the instantaneous energy consumption is carried out; third, given a performance function correlated with real instantaneous energy consumption and estimation value from ANN model, the Levenberg-Marquardt Backpropagation algorithm is implemented so that the weight and bias variables are updated along with the calculation of a Jacobian matrix of the performance function. Then iteratively, the ANN estimates the instantaneous energy consumption based on updated weights and biases at the next time step until the sum of squares reduces to some target error or the norm of the gradient becomes less than some predetermined value, during which the ANN-based instantaneous energy consumption

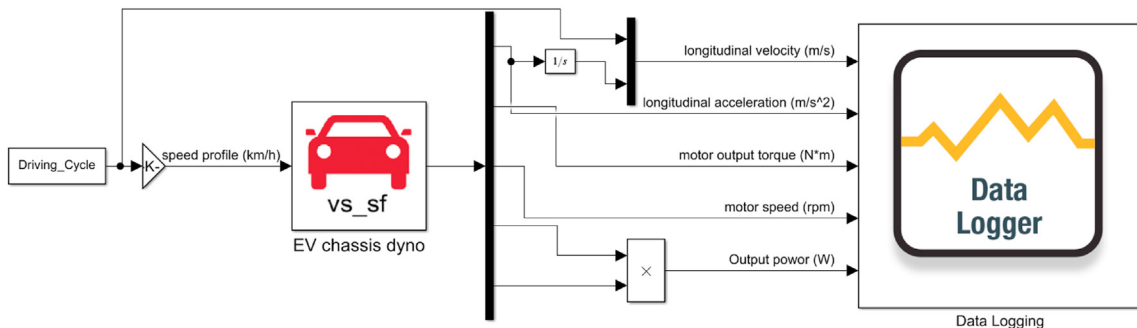


**Fig. 6.** Simulated EV chassis dynamometer.

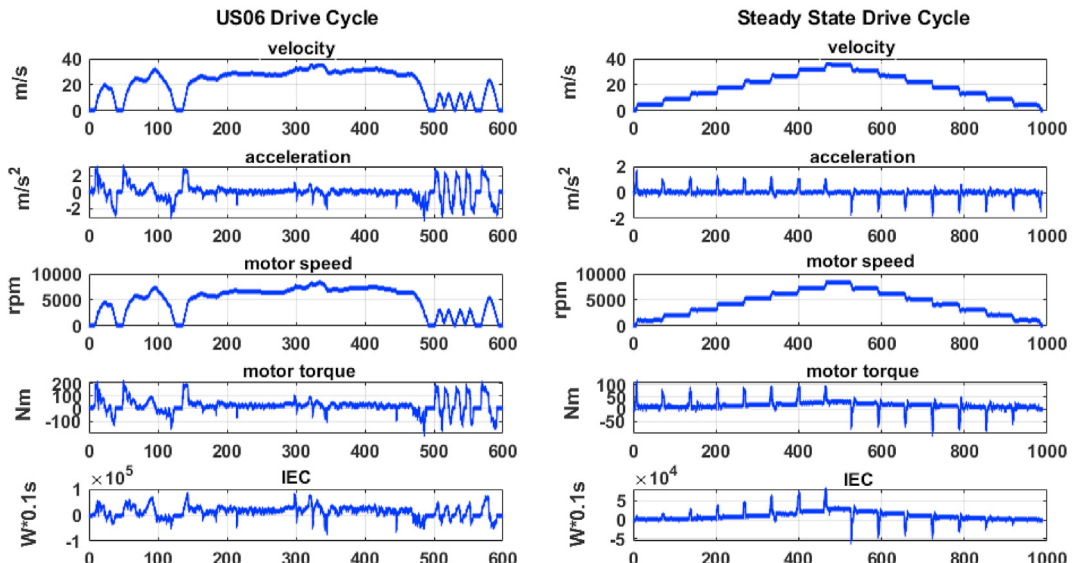


**Fig. 7.** Sample data of US06 drive cycle and steady-state drive cycle.

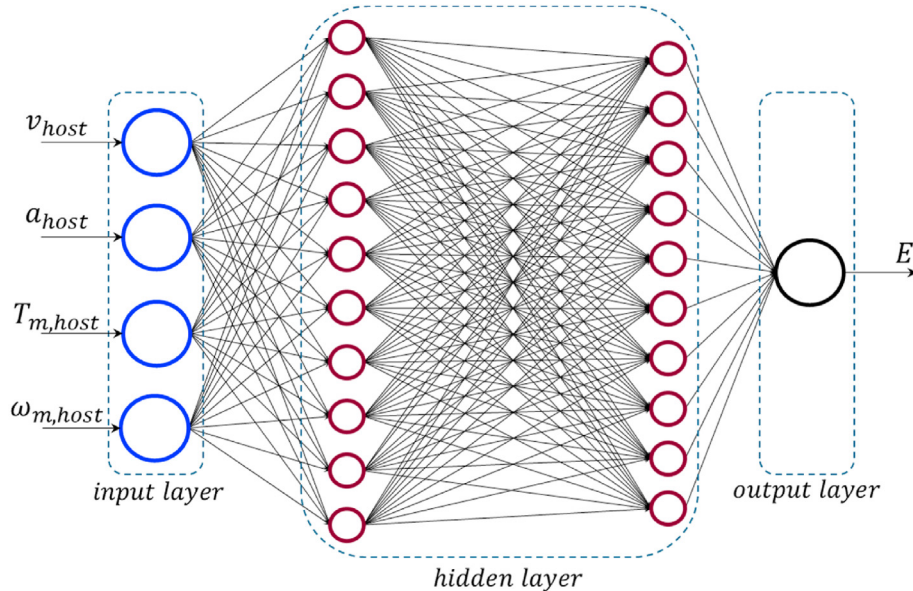


**Fig. 8.** The detailed structure of the proposed two hidden layers neural network.

model is well-trained. The system architecture with the proposed methodology is shown in Fig. 9.

As the basic element of the network, the neuron is the functional unit that conducts the mathematical calculation. A neuron accepts more than one input, which constitutes the input vector  $\mathbf{p} = [v_{host}, a_{host}, T_{m,host}, \omega_{m,host}]$ . Multiplied by a weight matrix  $\mathbf{W}$  and summed with a bias  $b$ , the net input  $n$  to the neuron is expressed as:

$$n = \sum_{i=1}^k w_i p_i + b = \mathbf{W} \cdot \mathbf{p} + b \quad (48)$$

Next, through the activation function  $f$ , the neuron output  $a$  is obtained by:

$$a = f(n) \quad (49)$$

In this paper, the rectified linear activation function is applied, which is expressed mathematically as:

$$f(x) = \begin{cases} 0 & (x < 0) \\ x & (x \geq 0) \end{cases} \quad (50)$$

As an approximation to Newton's method, the Levenberg-

Marquardt Backpropagation training algorithm is demonstrated in Fig. 10 [45,46].

Total layer  $\mathcal{L}$  is 3;  $\mathbf{a}_q^{\mathcal{L}}$ , namely  $E_q$ , is the estimated energy consumption output of the network when the  $q_{th}$  input,

$$\mathbf{p}_q = \begin{pmatrix} v_{host,q} \\ a_{host,q} \\ T_{m,host,q} \\ \omega_{m,host,q} \end{pmatrix}$$

denotes the error for the  $q_{th}$  input;  $\Delta w^{\ell}$  and  $\Delta b^{\ell}$  are the steepest descent algorithm parameters;  $\kappa$  refers to the learning rate;  $\delta^{\ell}$  refers to the sensitivity of the performance index  $PI$  to changes in the  $i$  th element of the net input in layer  $\ell$ ;  $PI(x)$  denotes that a function intended to be minimized with respect to the parameter vector  $x$ ;  $J(x)$  is the Jacobian matrix.

After training the neural network using the above Levenberg-Marquardt algorithm, the relationships between the outputs of the network and the targets are shown in Fig. 11. The regression values for training, testing, validation, and all dataset reach to 0.99, which means that the network outputs and the targets are precisely equal, and the neural network model is well trained.

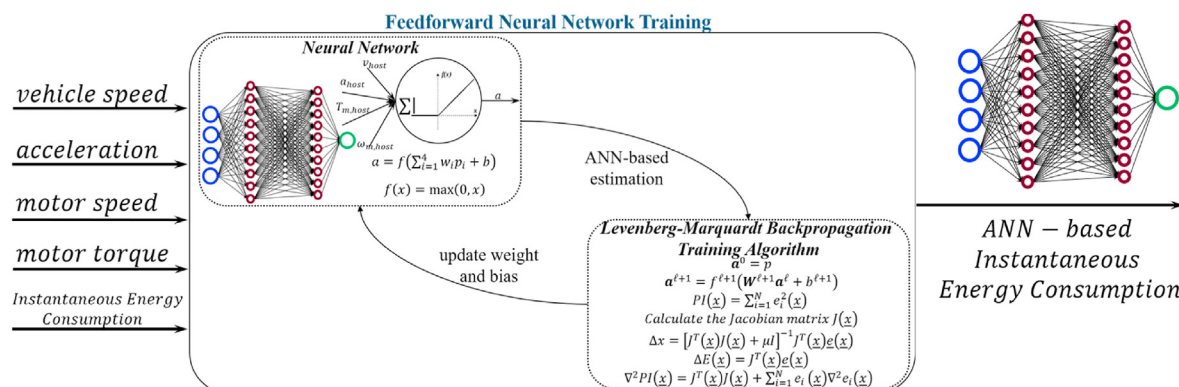


**Fig. 9.** Architecture of proposed Feedforward Neural Network Training Algorithm.

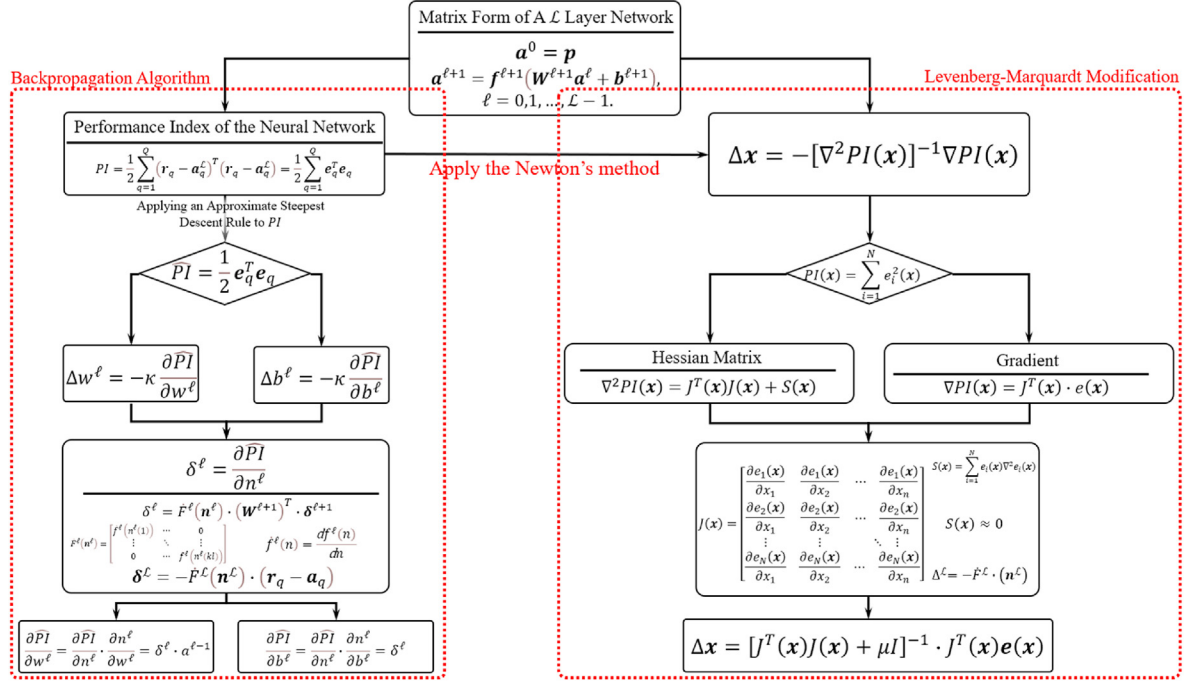


Fig. 10. Flow diagram of Levenberg-Marquardt Feedforward neural network training algorithm.

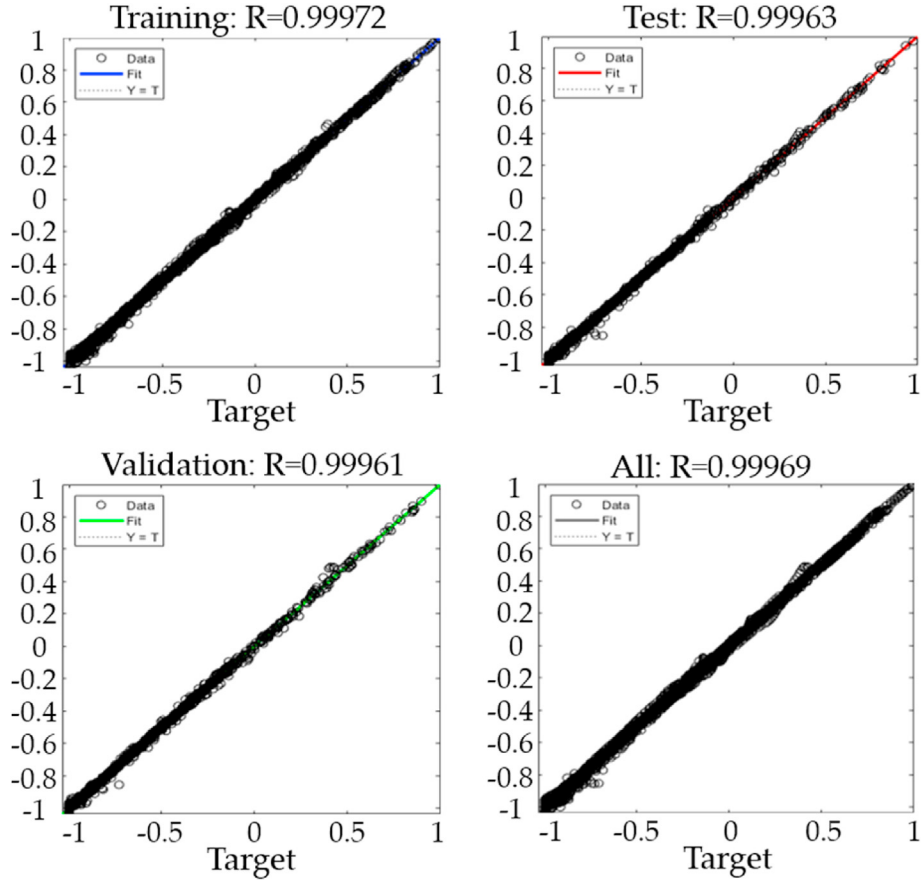


Fig. 11. Regression plots for training, testing, validation, and All.

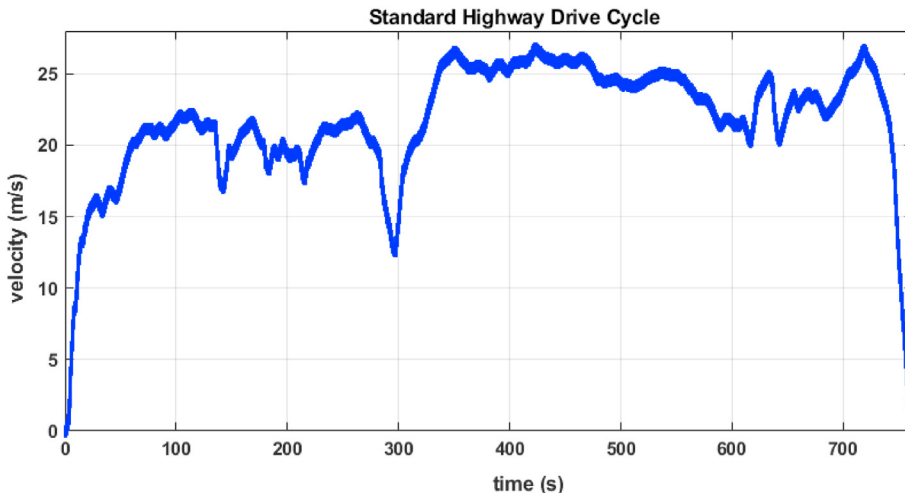


Fig. 12. Highway Drive Cycle velocity profile.

**Table 2**

The comparative validation result of ANN-IECM and EV-MFECM.

	MAPE(%)	MSE( $W \cdot 0.1s$ )
ANN-based IECM	1.25	$1.4231 \times 10^6$
EV-MFECM	3.20	$1.6850 \times 10^6$

Ultimately, the proposed ANN-based instantaneous energy consumption of the EV can be expressed as:

$$E(t) = f(v(t), a(t), T_m(t), \omega_m(t)) \quad (51)$$

where  $E(t)$  is the energy consumption for a time step ( $0.1s$ ).

A standard highway driving cycle, shown in Fig. 12, is adopted to validate the proposed instantaneous energy consumption model. Firstly, the standard highway drive cycle is used by the simulated EV chassis dynamometer platform in this research to generate the required input dataset for energy consumption estimation. To validate the accuracy of the proposed ANN-based instantaneous energy consumption estimation model (ANN-IECM), a multivariate fitting energy consumption model for electric vehicles (EV-MFECM)

from Ref. [47] is compared to show the estimation improvement. From Table 2, the comparative result shows that, under a standard Highway Drive Cycle, both the MSE (Mean Squared Error) and MAPE (Mean Absolute Percentage Error) values of proposed ANN-based IECM are lower than the corresponding values of baseline EV-MFECM, which indicates that estimation performance of ANN-based IECM is superior to the one based on statistical multivariate regression method. From Fig. 13, it is evident to see that both ANN-based IECM and EV-MFECM are capable of reflecting the trend of energy consumption under the Highway Drive Cycle. However, the proposed ANN-based IECM fits better and is more accurate than the baseline. The error of ANN-based IECM is closer to zero without any spikes. Besides, the EV-MFECM contains the polynomial combination, which makes it too complicated to be deployed in real applications. On the contrary, ANN-based IECM features an explicit model structure and is easy to encode into the hardware, making it more suitable for vehicle eco-driving optimization systems

### 3. Results and discussion

It is important to investigate the computational efficiency of MPC for real-time execution. The Simulations of the entire

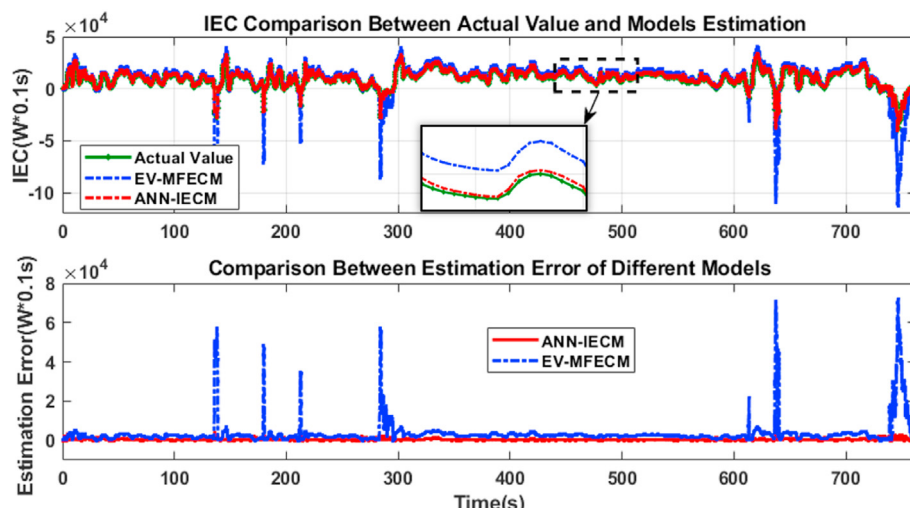
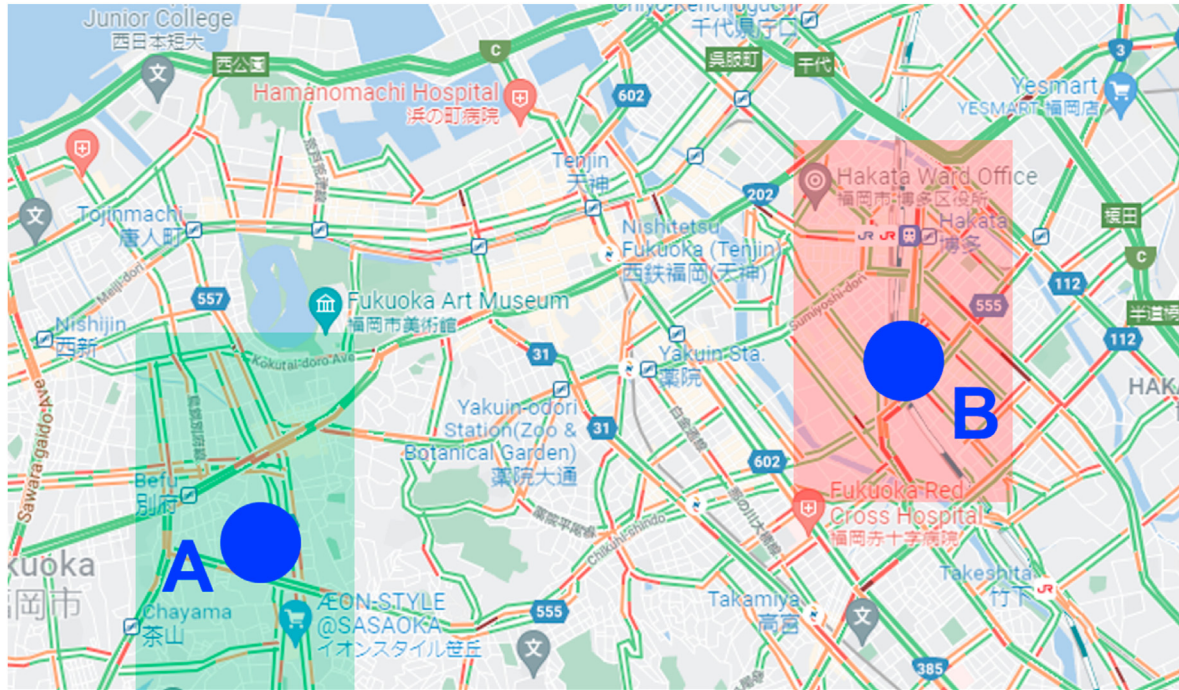


Fig. 13. Comparison between the estimation of models with the actual value and estimation error of different models.



**Fig. 14.** Location of suburban area A and urban area B for case studies.

**Table 3**

Specification of the simulated electric vehicle.

Equivalent total mass of the vehicle, $m_{eq}$	1260 kg
Single transmission ratio, $i_g$	2.06
Total mechanical efficiency of the driveline, $\eta_e$	0.95
Radius of the vehicle wheel, $r_w$	0.3 m
Frontal area of the vehicle, $A_f$	2.22 $m^2$
Rolling resistance coefficient, $c_r$	0.028
Aerodynamic drag coefficient, $C_D$	0.316

predictive cruise control are run on an Intel-Core-i7 CPU (3.60 GHz) and 8 GB memory. The computational time of 5.23 ms per sampling step can be obtained in MATLAB, which shows the real-time applicability of the proposed control system. To validate the proposed real-time dynamic predictive cruise control system and bear out the energy efficiency, two representative case studies are conducted with access to real traffic signal phasing and timing data in both suburban area A and urban area B in Fukuoka, Japan, under the different traffic systems, seen in the following map (see Fig. 14)

Real-time driving speed profile data acquisition is supported by MATLAB Mobile, by which built-in sensors on the smartphone in the vehicle can record the real-time driving data, such as acceleration, velocity, and position. Then, the sensor data can be streamed directly to the MathWorks Online Cloud for further application or analysis. Here, the sensor data are collected and used as the velocity and position of the preceding vehicle controlled by a human driver. Whether the preceding vehicle runs within range or not, the host vehicle deployed with the PCC system handles the driving task by dynamically switching to either the car-following-oriented MPC to track the preceding vehicle's velocity profile or to SPaT-oriented MPC to track the reference target velocity optimized by upcoming SPaT information. The related parameters used to model the electric vehicle are listed in Table 3.

### 3.1. Case study I

The first case study is conducted in the traffic system of a suburban area, shown in Fig. 15. From an ego-centric view, it is intuitive that the vehicle with PCC system needs to deal with the constraints from both the preceding vehicle and traffic signal light. This road section is located in the central residential area, which features an average traffic flow movement of 40–80 km/h, during off-peak hours. There are nine consecutive traffic signal lights on this road section, which cover 4.2 km in total; their positions were measured through Google Map. The baseline vehicle is controlled using the Intelligent Driver Model (IDM), which is a time-continuous car-following model [48]. It is the simplest complete and accident-free model producing realistic acceleration and car-following behavior in single-lane traffic situations. The mathematical description of the IDM is shown as follow:

$$\dot{v}_i = a_i \left[ 1 - \left( \frac{v_i}{v_{d,i}} \right)^\delta - \left( \frac{s^*(v_i, \Delta v)}{s_i} \right)^2 \right] \quad (52)$$

$$s^*(v_i, \Delta v) = s_s + h v_i + \frac{v_i \Delta v}{2 \sqrt{a_i b_i}}$$

where  $v_i$  and  $v_{d,i}$  are the current and desired velocities of the host vehicle  $i$ .  $\delta$  represents the acceleration exponent that feedbacks the driving aggressiveness of the vehicle.  $s_i$  denotes the current inter-vehicle distance.  $s^*(v_i, \Delta v)$  is the variable of the desired inter-vehicle distance, where  $s_s$  is the minimum safety distance and  $h$  is the constant time headway.  $\Delta v$  stands for the error between current velocity and desired velocity.  $a_i$  and  $b_i$  are the maximum and desired acceleration of the host vehicle, respectively.

As shown in Fig. 16, compared with the pure car-following algorithm IDM, the proposed PCC system can optimize the driving

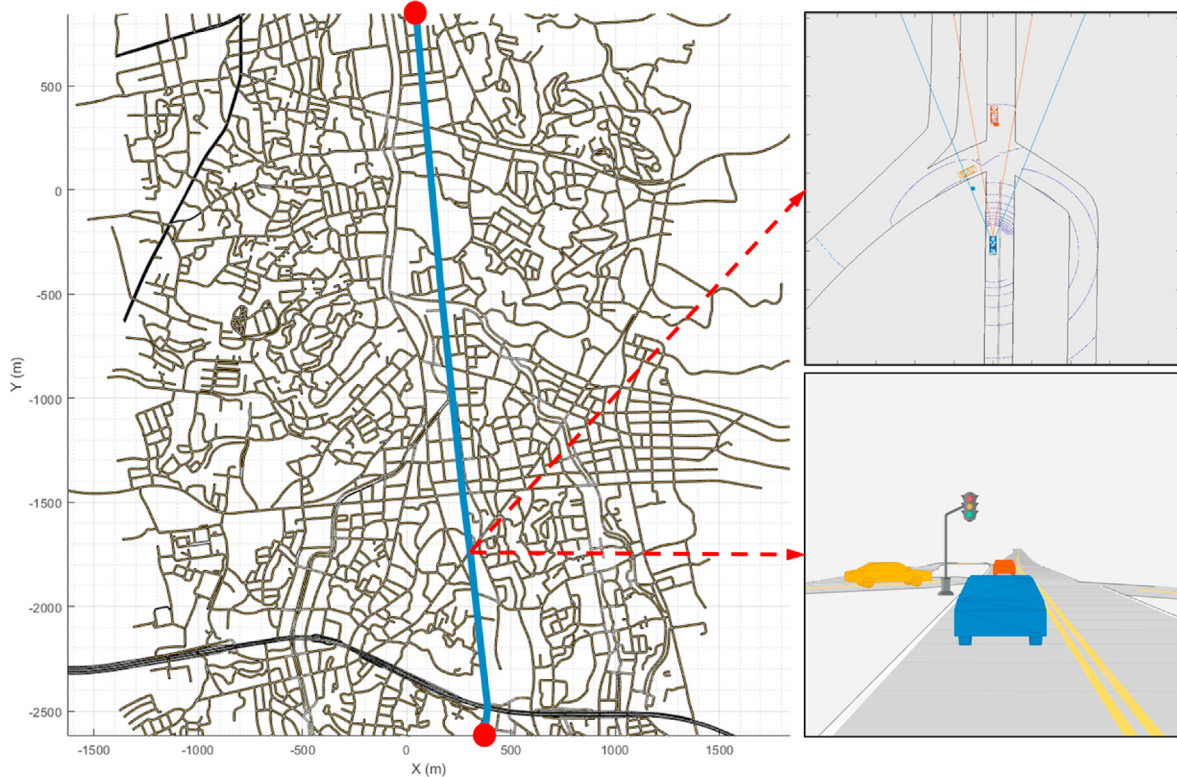


**Fig. 15.** Map of the road section in case study I and driving condition.

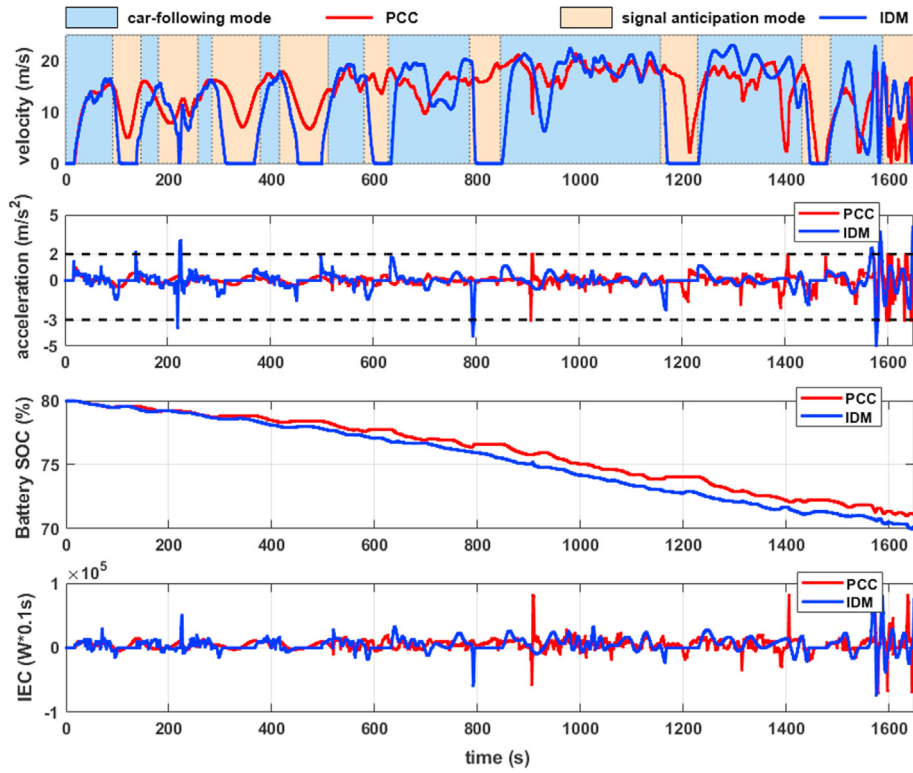


**Fig. 16.** Velocity, acceleration, battery SOC and the instantaneous energy consumption.

velocity based on the upcoming traffic SPaT information so that the host vehicle can pass the signalized intersection during the green

interval, which can save a lot of energy that could be consumed by frequent stop and go due to traffic signal lights. Benefit from

explicitly dealing with the constraints of the inputs and state variable using MPC, the acceleration of the host vehicle controlled by the proposed PCC system can be bounded within a certain range of preceding and the host vehicle in case study I.

The energy-saving performance can be directly seen from the final settled value of the battery SOC. The battery SOC of the vehicle controlled by IDM is 70.08%, while the car controlled by the PCC system still has the SOC of 70.98%. Based on the cumulative calculation of the energy consumption, 8.5% energy-saving rates can be achieved by PCC-based vehicle compared with IDM-based vehicle.

### 3.2. Case study II

The second simulation case study was conducted for the road in the urban area located in the core commercial district, which is shown in Fig. 17. The selected location in this case study is characterized by an average traffic flow movement of 30–50 km/h during off-peak hours, and 35 km/h during peak hours, which directly influences the running condition of the preceding vehicle. Seven traffic signal lights were considered in the SPaT data collection process. Assuming that only the host and preceding vehicles were operating during simulation, without considering the constraints of other vehicles, the host vehicle maintained a safe distance from the preceding vehicle using car-following-oriented MPC by 60s (see Fig. 18). After that, the preceding vehicle kept accelerating. It follows that the PCC system switched to the SPaT-oriented MPC to track the reference target velocity optimized by upcoming traffic SPaT information to avoid coming to a red interval. After experiencing a stop during the red interval for the preceding vehicle, the switch logic actuated the function of car-following-oriented MPC to track the preceding vehicle within the onboard sensor range from 180s to 320s. Subsequently, the preceding vehicle implemented a sharp deceleration. However, through managing the velocity of the host vehicle by the proposed PCC system, it successfully avoided the arrival at the signalized

intersection during the red interval. Fig. 18 right plot demonstrates the spacetime diagram comparing preceding and PCC-equipped host vehicles. The solid blue line represents the optimized trajectory passing each traffic signal light sequence through green intervals. By contrast, the preceding vehicle trajectory illustrated by the dotted red line encountered two-stop during red intervals.

Once getting into the high traffic flow from a low traffic flow situation, the car-following-oriented MPC is selected by the PCC system to track the preceding vehicle while maintaining a suitable inter-distance between two vehicles. Afterward, relative distance kept increasing due to the acceleration of the preceding vehicle, during which the host vehicle tracks the reference target speed optimized by upcoming traffic SPaT information. After a stop in front of a red interval from 720s to 735s, the preceding vehicle starts to keep accelerating. However, the host vehicle deploys by the proposed PCC system crosses the signalized intersection without any stop through managing the driving velocity. A sharp deceleration is implemented by the preceding vehicle because of the upcoming red interval from 870s to 890s, during which the host vehicle is controlled by the SPaT-oriented MPC controller to avoid encountering the red interval. From 965s, the host vehicle sharply accelerated to follow the preceding vehicle and maintained a suitable inter-distance. Until the end of 1000s, the SPaT-oriented MPC of the PCC system is selected again to track the reference target speed and successfully pass the signalized intersection with any stop. However, the preceding vehicle without any velocity optimization had to experience a stop at around 1090s. Fig. 18 right plot visualized the behavior of both host and preceding vehicles in a spacetime schematic. The energy savings rate for this case study reached a remarkable value of 15.6%.

### 3.3. Case study III

To evaluate the performance and applicability of the proposed PCC system working under high speed driving scenario and the transition from highway to urban road, another case study was

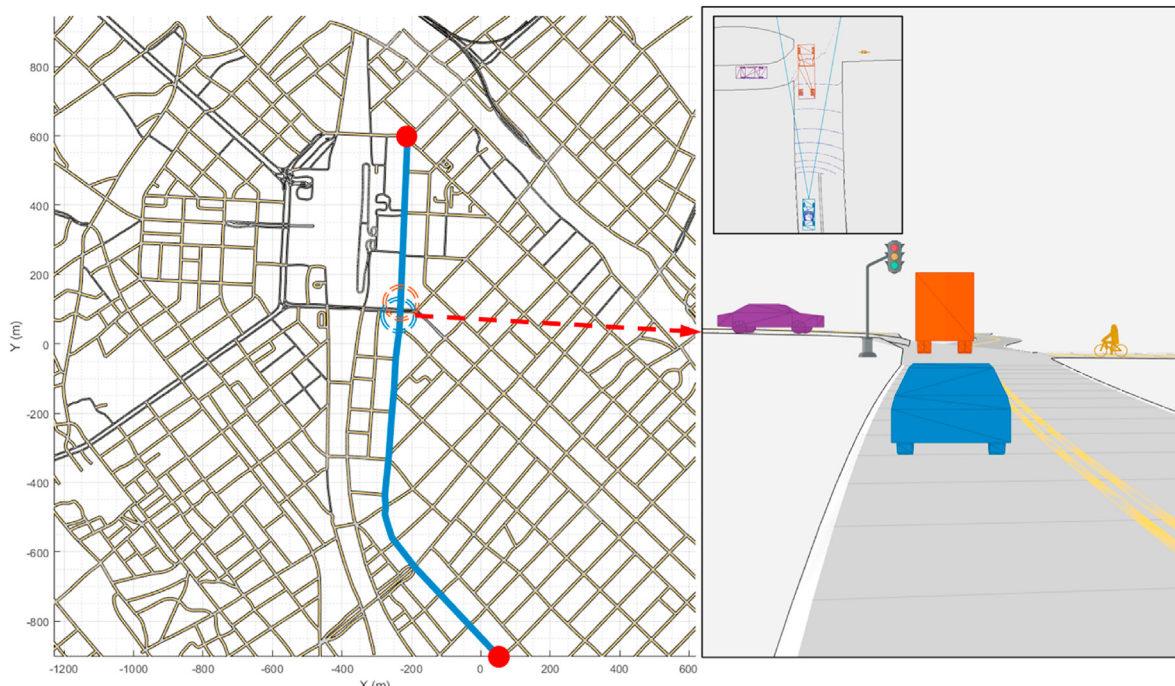


**Fig. 17.** Google Map of the road section for case study II.

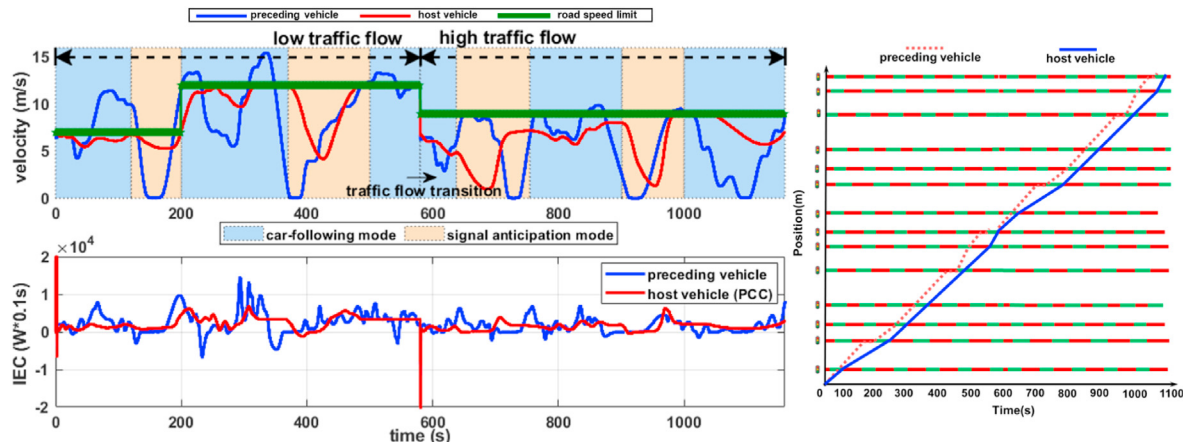


**Fig. 18.** Velocity and the instantaneous energy consumption of preceding and the host vehicle in case study II; Spacetime diagram with SPaT information comparing preceding and host vehicle with PCC system for case study II.

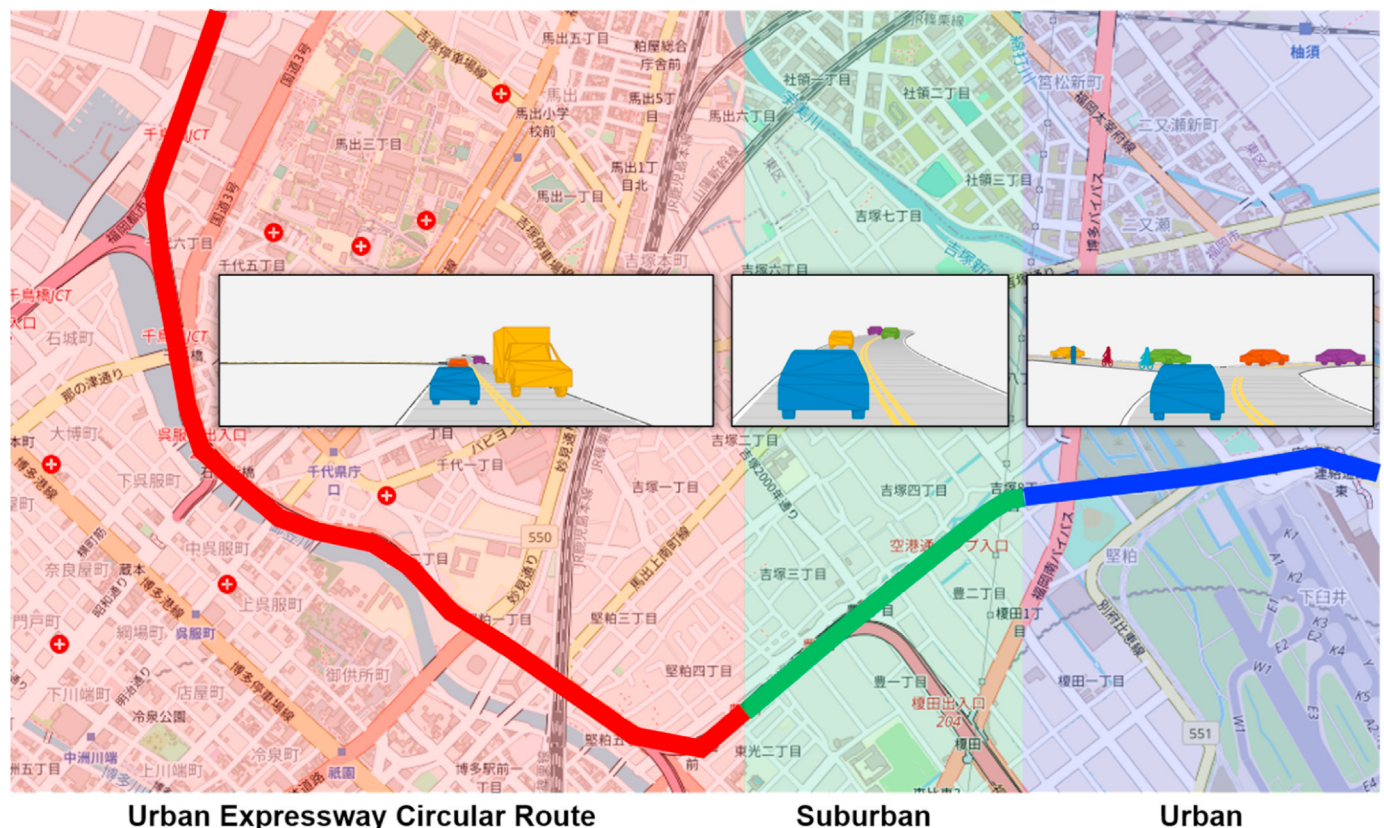


**Fig. 19.** Roadmap of the case study from the highway to urban area road.

conducted based on the real traffic and driving data collected in an area covering from urban expressway, suburban area to urban area, shown as Fig. 19. As seen from the driving situation demonstrated within Fig. 19, the car-following task is the main driving task on the highway. As the vehicle drives into the suburban area, more vehicles are merged into the main lane from ramps. In the urban area, due to the appearance of the traffic signal lights, the vehicle is required to execute the car-following task as well as the signal anticipation.

From the velocity profile part of Fig. 20, it is clear that the vehicle controlled by the proposed PCC system can work well and robustly

during the car-following scenario on the highway. As the velocity slows down in the suburban road, the PCC system can actively capture the traffic flow variation, executing the car-following at a slower speed range. After entering the urban road area, the PCC vehicle starts receiving the upcoming traffic SPaT information to optimize its driving velocity to avoid stopping in front of the red intervals. From Fig. 20 velocity profile in urban road area, it can be seen that the proposed PCC system optimized the velocity by six times while preceding vehicle driven by human driver inevitably stopped in front of the red intervals. Through the cumulative calculation from instantaneous energy consumption during this

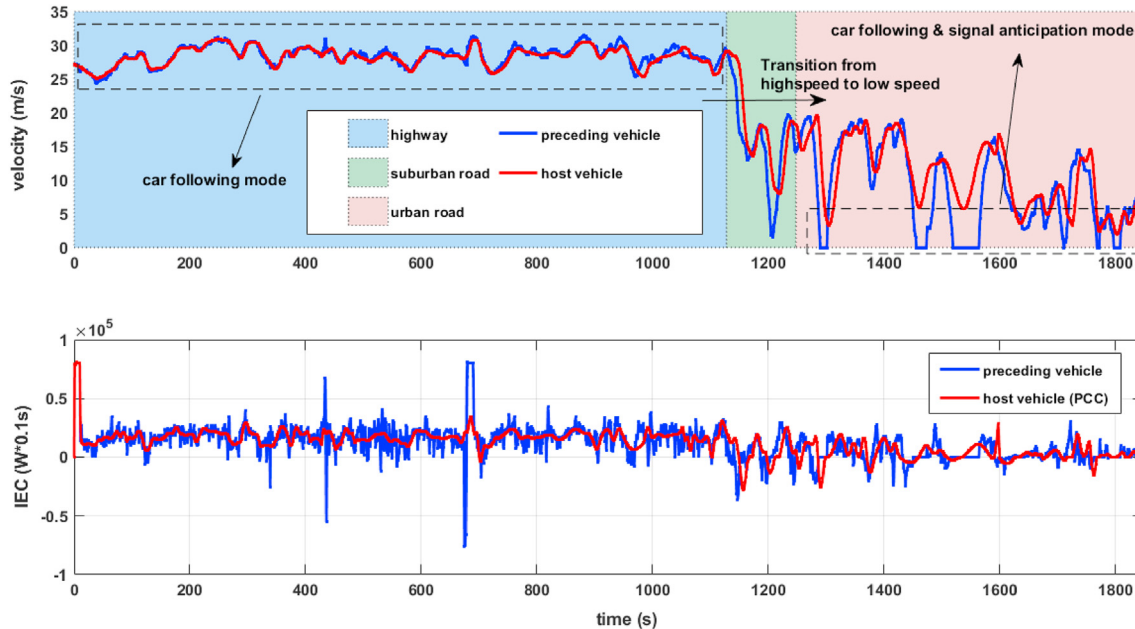


**Fig. 20.** Velocity and the instantaneous energy consumption of preceding and host vehicle in case study III.

trip, 7.2% energy-saving rates were achieved by the proposed PCC system.

To summarize, through the above three case studies, the host vehicle equipped with the proposed PCC system has achieved the energy savings rate range from 5.8% (Case study I) to 15.6% (Case study II), compared with the widely used car following algorithm – IDM, and the driver-controlled preceding vehicle. Through case study III, the adaptiveness of the proposed PCC system under a high driving speed situation can be validated.

#### 4. Conclusion

In this work, a real-time dynamic predictive cruise control system based on a bi-level model predictive control framework for electric vehicle eco-driving was proposed, in which either the car-following-oriented MPC with a novel VTH strategy or the SPaT-oriented MPC can be selected by a dynamic switch logic to realize the objective of eco-driving with optimal energy consumption in the synthetic transport systems. A novel ANN-based instantaneous energy consumption model was developed to quantify the energy consumption in each operating condition. The proposed control system was evaluated using the real traffic system and SPaT data through three case studies. The potential of energy saving in the traffic system of the suburban and urban areas during off-peak and peak hours was estimated at 8.5% and 15.6%, respectively. A road condition transitional-oriented case study was designed, which validated the adaptiveness of the proposed PCC system working under either low speed urban area or highway. The results highlighted the importance of the proposed system in minimizing the energy consumption for electric vehicles and relieving the energy and environmental burden from the road transportation sector. The development of the real-time dynamic PCC system is important not only from the point of view of reducing energy consumption and environmental pollutants, but also managing the charging schedule of EVs, through extending the state of charge (SoC) of the vehicle. Furthermore, as an enhancement of the current ACC system, the proposed PCC system can fully take into account the local information (velocity of the preceding vehicle) and global information

(speed limits of particular road section, SPaT information) utilizing a wireless or Cloud-based V2I and V2V communication technology, which can inspire the development of next-generation intelligent transport system.

#### Credit author statement

Zifei Nie: Conceptualization, Methodology, Data collection, Software, Investigation, Writing – original draft. Hooman Farzaneh: Conceptualization, Supervision, Reviewing and Editing.

#### Declaration of competing interest

The authors declare that they have no known competing financial interests or personal relationships that could have appeared to influence the work reported in this paper.

#### Acknowledgments

This research was supported by the Kyushu Natural Energy Promotion Organization.

#### Nomenclature

$d_{rel}$	inter-distance between host and the preceding vehicle
$m$	
$d_{limit}$	onboard sensor detection range $m$
$d_{TL}$	relative distance to the upcoming signalized intersection $m$
$d_{TL,max}$	maximum relative distance to the upcoming signalized intersection $m$
$d_{TL,limit}$	limit relative distance to the upcoming signalized intersection $m$
$E$	instantaneous energy consumption of the host vehicle $W \cdot 0.1s$
$v_{host}$	velocity of the host vehicle $m/s$
$v_{min}$	physical minimum limitation of vehicle velocity $m/s$
$v_{max}$	physical maximum limitation of vehicle velocity $m/s$

$v_{preceding}$	velocity of the preceding vehicle $m/s$
$v_{rel}$	relative velocity between host and the preceding vehicle $m/s$
$a_{host}$	acceleration of host vehicle $m/s^2$
$a_{min}$	physical minimum limitation of acceleration $m/s^2$
$a_{max}$	physical maximum limitation of acceleration $m/s^2$
$j$	jerk $m/s^3$
$J_{min}$	minimum limitation of the jerk $m/s^3$
$J_{max}$	maximum limitation of the jerk $m/s^3$
$T_m$	motor torque $N\cdot m$
$T_{m,max}$	physical maximum limitation of motor torque $N\cdot m$
$\omega_m$	motor speed $rpm$
$\omega_{m,max}$	physical maximum limitation of motor speed $rpm$
$v_{target}$	optimized reference target vehicle velocity $m/s$
$\varepsilon_1, \varepsilon_2, \varepsilon_3$	relaxation factor –
$\varphi_1, \varphi_2, \varphi_3$	weighting factor –
$i$	current control time step $s$
$N_e$	control horizon $s$
$m_{eq}$	equivalent total mass of the vehicle $kg$
$i_g$	gear ratio of single transmission of EV –
$\eta_e$	total mechanical efficiency of driveline –
$r_w$	radius of the vehicle wheel $m$
$c_r$	rolling resistance coefficient –
$g$	gravitational acceleration $m/s^2$
$\theta$	road gradient $degree(^{\circ})$
$A_f$	frontal area of the host vehicle $m^2$
$C_D$	aerodynamic drag coefficient –
$D_{safe}$	dynamic safe distance between host and the preceding vehicle $m$
$d_{min}$	minimum inter-distance between host and preceding vehicle when they are motionless $m$
$\tau_1, \tau_2, \tau_3$	constant values greater than zero –
$CTH$	constant time headway $s$
$VTH$	variable time headway $s$
$v_{limits}$	vehicle limitation on a certain road section $m/s$
$U_{trigonometric speed profile}$	control command derived from trigonometric speed profile –
$u_{driver set}$	control command derived from driver set speed –
$r_i$	start time of the red interval of the nearest upcoming traffic signal light $s$
$g_i$	start time of the green interval of the nearest upcoming traffic signal light $s$
$u^1(i), u^2(i), \dots, u^k(i)$	control sequence computed from MPC controller for each time step –
$\lambda$	time lag corresponding to the finite bandwidth of vehicle dynamic response –
$T_s$	sampling time period $s$
$v_{avg}$	possible average host velocity required to reach the target stop bar at a specific time instant $m/s$
$v_{curr}$	current host vehicle velocity $m/s$
$t_{arr}$	time required to reach the target stop bar $s$
$v_r$	difference between the $v_{curr}$ and $v_{avg}$ $m/s$
$p, q$	determinants to regulate the jerk when planning to implement a stop –
$F_{trac}$	traction force $N$
$F_{res}$	collective resistance forces $N$
$F_{roll}$	rolling resistance force $N$
$F_{aero}$	aerodynamic drag force $N$
$F_g$	gradient resistance force $N$
$W$	weight matrix –
$b$	bias –
$e_q$	error for the $q$ th input –

$\Delta \mathbf{w}^\ell$	$\Delta \mathbf{b}^\ell$ steepest descent algorithm parameters –
$\kappa$	learning rate –
$\delta^\ell$	sensitivity of the performance index $PI$ to changes in the $i$ th element of the net input in layer $\ell$ –
$PI(x)$	performance index intended to be minimized with respect to the parameter vector $x$ –
$J(x)$	Jacobian matrix –
$A_t$	actual energy consumption each time step $W \cdot 0.1s$
$E_t$	estimated energy consumption each time step $W \cdot 0.1s$
$E_{savings}$	energy savings $W \cdot 0.1s$
$T$	entire simulation time $s$

## References

- [1] IEA. Tracking transport 2020. Paris: IEA; 2020. <https://www.iea.org/reports/tracking-transport-2020>.
- [2] United Nations. Sustainable development goal 11: make cities inclusive, safe, resilient and sustainable. <https://sdgs.un.org/topics/sustainable-transport>.
- [3] IEA. Global EV outlook 2020. Paris: IEA; 2020. <https://www.iea.org/reports/global-ev-outlook-2020>.
- [4] Schwarzkopf A, Leipnik R. Control of highway vehicles for minimum fuel consumption over varying terrain. Transport Res 1977;11(4):279–86. [https://doi.org/10.1016/0041-1647\(77\)90093-4](https://doi.org/10.1016/0041-1647(77)90093-4).
- [5] Hellström E, Ivarsson M, Åslund J, Nielsen L. Look-ahead control for heavy trucks to minimize trip time and fuel consumption. Control Eng Pract 2009;17(2):245–54. <https://doi.org/10.1016/j.conengprac.2008.07.005>.
- [6] Ozatay E, Ozguner U, Michelini J, Filev D. Analytical solution to the minimum energy consumption based velocity profile optimization problem with variable road grade. IFAC Proc Vol 2014;47(3):7541–6. <https://doi.org/10.3182/20140824-6-za-1003.01360>.
- [7] Ding F, Jin H. On the optimal speed profile for eco-driving on curved roads. IEEE Trans Intell Transport Syst 2018;19(12):4000–10. <https://doi.org/10.1109/tits.2018.2795602>.
- [8] Shen D, Karbowski DA, Rousseau A. Highway eco-driving of an electric vehicle based on minimum principle. In: 2018 IEEE vehicle power and propulsion conference (VPPC); 2018. <https://doi.org/10.1109/vppc.2018.8605032>.
- [9] Saboohi Y, Farzaneh H. Model for developing an eco-driving strategy of a passenger vehicle based on the least fuel consumption. Appl Energy 2009;86(10):1925–32. <https://doi.org/10.1016/j.apenergy.2008.12.017>.
- [10] Weißmann A, Görge D, Lin X. Energy-optimal adaptive cruise control combining model predictive control and dynamic programming. Control Eng Pract 2018;72:125–37. <https://doi.org/10.1016/j.conengprac.2017.12.001>.
- [11] Huang K, Yang X, Lu Y, Mi CC, Kondapudi P. Ecological driving system for connected/Automated vehicles using a two-stage control hierarchy. IEEE Trans Intell Transport Syst 2018;19(7):2373–84. <https://doi.org/10.1109/tits.2018.2813978>.
- [12] Asadi B, Vahidi A. Predictive cruise control: utilizing upcoming traffic signal information for improving fuel economy and reducing trip time. IEEE Trans Control Syst Technol 2011;19(3):707–14. <https://doi.org/10.1109/tcst.2010.2047860>.
- [13] Kamal MA, Mukai M, Murata J, Kawabe T. Model predictive control of vehicles on urban roads for improved fuel economy. IEEE Trans Control Syst Technol 2013;21(3):831–41. <https://doi.org/10.1109/tcst.2012.2198478>.
- [14] Mahler G, Vahidi A. An optimal velocity-planning scheme for vehicle energy efficiency through probabilistic prediction of traffic-signal timing. IEEE Trans Intell Transport Syst 2014;15(6):2516–23. <https://doi.org/10.1109/tits.2014.2319306>.
- [15] De Nunzio G, De Wit CC, Moulin P, Di Domenico D. Eco-driving in urban traffic networks using traffic signals information. Int J Robust Nonlinear Control 2015;26(6):1307–24. <https://doi.org/10.1002/rnc.3469>.
- [16] Meng X, Cassandra CG. A real-time optimal eco-driving approach for autonomous vehicles crossing multiple signalized intersections. In: 2019 American control conference (ACC); 2019. <https://doi.org/10.23919/acc.2019.8814864>.
- [17] Bae S, Kim Y, Guanetti J, Borrelli F, Moura S. Design and implementation of ecological adaptive cruise control for autonomous driving with communication to traffic lights. In: 2019 American control conference (ACC); 2019. <https://doi.org/10.23919/acc.2019.8814905>.
- [18] Yang H, Almutairi F, Rakha H. Eco-driving at signalized intersections: a multiple signal optimization approach. IEEE Trans Intell Transport Syst 2020: 1–13. <https://doi.org/10.1109/tits.2020.2978184>.
- [19] Chen H, Guo L, Ding H, Li Y, Gao B. Real-time predictive cruise control for eco-driving taking into account traffic constraints. IEEE Trans Intell Transport Syst 2018;1–11. <https://doi.org/10.1109/tits.2018.2868518>.
- [20] Nie Z, Farzaneh H. Adaptive cruise control for eco-driving based on model predictive control algorithm. Appl Sci 2020;10(15):5271. <https://doi.org/10.3390/app10155271>.
- [21] Zhou M, Yu Y, Qu X. Development of an efficient driving strategy for

- connected and automated vehicles at signalized intersections: a reinforcement learning approach. *IEEE Trans Intell Transport Syst* 2020;21(1):433–43. <https://doi.org/10.1109/tits.2019.2942014>.
- [22] Li SE, Peng H, Li K, Wang J. Minimum fuel control strategy in automated car-following scenarios. *IEEE Trans Veh Technol* 2012;61(3):998–1007. <https://doi.org/10.1109/tvt.2012.2183401>.
- [23] Vajedi M, Azad NL. Ecological adaptive cruise controller for plug-in hybrid electric vehicles using nonlinear model predictive control. *IEEE Trans Intell Transport Syst* 2016;17(1):113–22. <https://doi.org/10.1109/tits.2015.2462843>.
- [24] Ojeda LL, Han J, Sciarretta A, De Nunzio G, Thibault L. A real-time eco-driving strategy for automated electric vehicles. In: 2017 IEEE 56th annual conference on decision and control (CDC); 2017. <https://doi.org/10.1109/cdc.2017.8264061>.
- [25] Yue H. Mesoscopic fuel consumption and emission modeling. 2008 [Doctoral dissertation].
- [26] Zhou M, Jin H. Development of a transient fuel consumption model. *Transport Res Transport Environ* 2017;51:82–93. <https://doi.org/10.1016/j.trd.2016.12.001>.
- [27] Diaz Alvarez A, Serradilla Garcia F, Naranjo JE, Anaya JJ, Jimenez F. Modeling the driving behavior of electric vehicles using smartphones and neural networks. *IEEE Intell Transport Syst Magaz* 2014;6(3):44–53. <https://doi.org/10.1109/mitss.2014.2322651>.
- [28] Modi S, Bhattacharya J, Basak P. Estimation of energy consumption of electric vehicles using deep Convolutional neural network to reduce driver's range anxiety. *ISA (Instrum Soc Am) Trans* 2020;98:454–70. <https://doi.org/10.1016/j.isatra.2019.08.055>.
- [29] Yang C, Wang M, Wang W, Pu Z, Ma M. An efficient vehicle-following predictive energy management strategy for PHEV based on improved sequential quadratic programming algorithm. *Energy* 2021;219:119595. <https://doi.org/10.1016/j.energy.2020.119595>.
- [30] Hu X, Zhang X, Tang X, Lin X. Model predictive control of hybrid electric vehicles for fuel economy, emission reductions, and inter-vehicle safety in car-following scenarios. *Energy* 2020;196:117101. <https://doi.org/10.1016/j.energy.2020.117101>.
- [31] Ma F, Yang Y, Wang J, Liu Z, Li J, Nie J, Shen Y, Wu L. Predictive energy-saving optimization based on nonlinear model predictive control for cooperative connected vehicles platoon with V2V communication. *Energy* 2019;189:116120. <https://doi.org/10.1016/j.energy.2019.116120>.
- [32] Wu Y, Tan H, Peng J, Zhang H, He H. Deep reinforcement learning of energy management with continuous control strategy and traffic information for a series-parallel plug-in hybrid electric bus. *Appl Energy* 2019;247:454–66. <https://doi.org/10.1016/j.apenergy.2019.04.021>.
- [33] Shi D, Liu S, Cai Y, Wang S, Li H, Chen L. Pontryagin's minimum principle based fuzzy adaptive energy management for hybrid electric vehicle using real-time traffic information. *Appl Energy* 2021;286:116467. <https://doi.org/10.1016/j.apenergy.2021.116467>.
- [34] Lin Q, Li SE, Xu S, Du X, Yang D, Li K. Eco-driving operation of connected vehicle with V2I communication among multiple signalized intersections. *IEEE Intell Transport Syst Magaz* 2021;13(1):107–19. <https://doi.org/10.1109/mitss.2020.3014113>.
- [35] Jia Y, Jibrin R, Gorges D. Energy-optimal adaptive cruise control for electric vehicles based on linear and nonlinear model predictive control. *IEEE Trans Veh Technol* 2020;69(12):14173–87. <https://doi.org/10.1109/tvt.2020.3044265>.
- [36] Wang Z, Wu G, Barth MJ. Cooperative eco-driving at signalized intersections in a partially connected and automated vehicle environment. *IEEE Trans Intell Transport Syst* 2020;21(5):2029–38. <https://doi.org/10.1109/tits.2019.2911607>.
- [37] Ma F, Yang Y, Wang J, Li X, Wu G, Zhao Y, Wu L, Aksun-Guvenc B, Guvenc L. Eco-driving-based cooperative adaptive cruise control of connected vehicles platoon at signalized intersections. *Transport Res Transport Environ* 2021;92:102746. <https://doi.org/10.1016/j.trd.2021.102746>.
- [38] Zhao S, Zhang K. Online predictive connected and automated eco-driving on signalized arterials considering traffic control devices and road geometry constraints under uncertain traffic conditions. *Transp Res Part B Methodol* 2021;145:80–117. <https://doi.org/10.1016/j.trb.2020.12.009>.
- [39] n.d. Swaroop D, Rajagopal K. A review of constant time headway policy for automatic vehicle following. In: 2001 IEEE intelligent transportation systems. Proceedings (cat. No.01TH8585). ITSC; 2001. <https://doi.org/10.1109/itsc.2001.948631>.
- [40] Barth M, Mandava S, Boriboonsomsin K, Xia H. Dynamic ECO-driving for arterial corridors. In: 2011 IEEE forum on integrated and sustainable transportation systems; 2011. <https://doi.org/10.1109/fists.2011.5973594>.
- [41] Zhou M, Jin H, Wang W. A review of vehicle fuel consumption models to evaluate eco-driving and eco-routing. *Transport Res Transport Environ* 2016;49:203–18. <https://doi.org/10.1016/j.trd.2016.09.008>.
- [42] Zhou M, Jin H. Development of a transient fuel consumption model. *Transport Res Transport Environ* 2017;51:82–93. <https://doi.org/10.1016/j.trd.2016.12.001>.
- [43] n.d. Argonne national laboratory. Argonne National Laboratory Argonne National Laboratory <https://www.anl.gov/es/downloadable-dynamometer-database>.
- [44] Kürková V. Kolmogorov's theorem and multilayer neural networks. *Neural Network* 1992;5(3):501–6. [https://doi.org/10.1016/0893-6080\(92\)90012-8](https://doi.org/10.1016/0893-6080(92)90012-8).
- [45] Marquardt DW. An algorithm for least-squares estimation of nonlinear parameters. *SIAM J Appl Math* 1963;11:431–41. <https://doi.org/10.1137/0111030>.
- [46] Hagan MT, Menhaj MB. Training feedforward networks with the Marquardt algorithm. *IEEE Trans Neural Network* 1994;5(6):989–93. <https://doi.org/10.1109/72.329697>.
- [47] Yu, Y.; Li, Y.; Liang, Z.; Liao, G. Modeling of transient energy consumption model of electric vehicle based on data mining. In Proceedings of the society of automotive engineers of automotive engineering conference, shanghai, China, 21–22 may 2019; pp. 277–283.
- [48] Treiber M, Kesting A. Traffic flow dynamics: data, models and simulation. Springer Science & Business Media; 2012.